Two-dimensional MXene and Molybdenum Disulphide (MoS₂) for the Removal of Hexavalent Chromium Cr(VI) from Water: A Comparative Study

By

Asma Maqsood

(Registration No: 00000363600)

Institute of Environmental Sciences & Engineering

School of Civil & Environmental Engineering

National University of Sciences & Technology (NUST)

Islamabad, Pakistan

(2024)

Two-dimensional MXene and Molybdenum Disulphide (MoS₂) for the Removal of Hexavalent Chromium Cr(VI) from Water: A Comparative Study

By

Asma Maqsood

(Registration No: 00000363600)

A thesis submitted in partial fulfillment of the requirements for the

degree of

Master of Science in
Environmental Engineering

Supervisor: Dr. Musharib Khan

Co-supervisor: Dr. Waheed Miran

Institute of Environmental Sciences & Engineering

School of Civil & Environmental Engineering

National University of Sciences & Technology (NUST)

Islamabad, Pakistan

(2024)

THESIS ACCEPTANCE CERTIFICATE

Certified that final copy of MS Thesis written by Ms. Asma Maqsood (Registration No. 363600), of SCEE (IESE) has been vetted by undersigned, found complete in all respects as per NUST Statutes/ Regulations/Masters Policy, is free of plagiarism, errors, and mistakes and is accepted as partial fulfillment for award of Master's degree. It is further certified that necessary amendments as pointed out by GEC members and foreign/ local evaluators of the scholar have also been incorporated in the said thesis.

Signature: _____

Name of Supervisor _____Dr. Musharib Khan_____

Date: ___28 March 2024___

Signature (Co-supervisor): _____ 28/03/2024

Date: ___28/03/2024.___

Dr. Muhammad Ali Inam
Assistant Professor
HoD Environmental Engineering
SCEE (IESE), NUST
H-12 Islamabad

Signature (HoD): _____

Date: ___28-03-2024___

Signature (Associate Dean): _____

Prof. Dr. Imran Hashmi
Associate Dean
IESE (SCEE) NUST Islamabad

Date: ___28-03-2024___

Signature (Principal & Dean SCEE): _____

PROF DR MUHAMMAD IRFAN
Principal & Dean
SCEE, NUST

Date: ___0 2 APR 2024___

National University of Sciences & Technology

MS THESIS WORK

We hereby recommend that the dissertation prepared under our supervision by Asma Maqsood Titled: "Two-dimensional MXene and Molybdenum Disulphide (MoS₂) for the Removal of Hexavalent Chromium Cr(VI) from Water: A Comparative Study be accepted in partial fulfillment of the requirements for the award of MS degree.
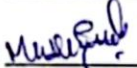
Examination Committee Members
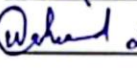
1. Dr. Muhammad Arshad   Signature: _____

2. Dr. Hassan Anwer   Signature: _____ 29·03·24

Supervisor: Dr. Musharib Khan   Signature: _____ 28/03/2024

Co-supervisor: Dr Waheed Miran Signature: _____ 28/03/2024,

Signature HoD: _____ Dr. Muhammad Ali Inam
                             Assistant Professor Date: 28-03-2024
                    HoD Environmental Engineering
                        SCEE (IESE), NUST
                          H-12 Islamabad

COUNTERSIGNED

Principal & Dean SCEE: _____   Date: 02 APR 2024
       PROF DR MUHAMMAD IRFAN
       Principal & Dean
       SCEE, NUST

CERTIFICATE OF APPROVAL

This is to certify that the research work presented in this thesis, entitled "Two-dimensional MXene and Molybdenum Disulphide (MoS$_2$) for the Removal of Hexavalent Chromium Cr(VI) from Water: A Comparative Study" was conducted by Ms. Asma Maqsood under the supervision of Dr. Musharib Khan.

No part of this thesis has been submitted anywhere else for any other degree. This thesis is submitted to the Institute of Environmental Sciences and Engineering in partial fulfillment of the requirements for the degree of Master of Science in Field of Environmental Engineering.

School of Civil and Environmental Engineering, National University of Sciences and Technology, Islamabad.

Student Name: Asma Maqsood   Signature: _____

Guidance and Examination Committee:

    a) Dr. Muhammad Arshad   Signature: _____
       Professor,
       SCEE(IESE), NUST

    b) Dr. Hassan Anwer   Signature: _____
       Assistant Professor,
       SCEE(IESE), NUST

Supervisor : Dr. Musharib Khan   Signature: _____ 28/03/2024

Co-supervisor: Dr Waheed Miran   Signature: _____ 28/3/2024

    Dr. Muhammad Ali Inam
    Assistant Professor
HoD: Dr. Muhammad Ali Inam Environmental Engineering   Signature: _____ 28/03/2024
    SCEE (IESE), NUST
    H-12 Islamabad

    Prof. Dr. Imran Hashmi
Associate Dean : Dr. Imran Hashmi   Associate Dean   Signature: _____ 01/04/2024
    IESE (SCEE) NUST Islamabad

Principal & Dean SCEE   Signature: _____

    PROF DR MUHAMMAD IRFAN
    Principal & Dean
    SCEE, NUST

AUTHOR'S DECLARATION

I Asma Maqsood hereby state that my MS thesis titled "Two-dimensional MXene and Molybdenum Disulphide (MoS$_2$) for the Removal of Hexavalent Chromium Cr(VI) from Water: A Comparative Study" is my own work and has not been submitted previously by me for taking any degree from National University of Sciences and Technology, Islamabad or anywhere else in the country/ world.

At any time if my statement is found to be incorrect even after I graduate, the university has the right to withdraw my MS degree.

Name of Student:_____ Asma Maqsood _____

Date: _____ 28-March, 2024 _____

PLAGIARISM UNDERTAKING

I solemnly declare that research work presented in the thesis titled "Two-dimensional MXene and Molybdenum Disulphide (MoS$_2$) for the Removal of Hexavalent Chromium Cr(VI) from Water: A Comparative Study" is solely my research work with no significant contribution from any other person. Small contribution/ help wherever taken has been duly acknowledged and that complete thesis has been written by me.

I understand the zero tolerance policy of the HEC and National University of Sciences and Technology (NUST), Islamabad towards plagiarism. Therefore, I as an author of the above titled thesis declare that no portion of my thesis has been plagiarized and any material used as reference is properly referred/cited.

I undertake that if I am found guilty of any formal plagiarism in the above titled thesis even after award of MS degree, the University reserves the rights to withdraw/revoke my MS degree and that HEC and NUST, Islamabad has the right to publish my name on the HEC/University website on which names of students are placed who submitted plagiarized thesis.

Student Signature: _____

Name: _____ Asma Maqsood _____

DEDICATION

To my parents, whose unwavering love, sacrifices, and endless support have been my guiding light and source of strength. Your encouragement and belief in my abilities have been the driving force behind my pursuit of knowledge and excellence.

To my siblings, for being my constant companions, cheerleaders, and pillars of support throughout this journey. Your understanding, patience, and encouragement have been a source of immense comfort and motivation.

You have been my rock, my inspiration, and my greatest blessings. This thesis is a testament to the love, guidance, and sacrifices you have made to ensure my success. I dedicate this work to you with all my heart and gratitude.

May Allah bless you all with happiness, health, and prosperity, and may He reward you abundantly for all that you have done for me.

ACKNOWLEDGEMENTS

TABLE OF CONTENTS

LIST OF FIGURES

LIST OF TABLES

ABSTRACT

Chromium is one of the most typical heavy metal pollutants that is genotoxic, carcinogenic and accumulates in plant and animal bodies. The use of emerging materials for efficient removal of chromium is in high demand. MXene and MoS_2 were employed in this investigation to extract hexavalent chromium (Cr(VI)). The pseudo second order kinetic model described the adsorption of Cr(VI) on MXene and MoS_2. In the meanwhile, the Freundlich and Langmuir Isotherm models best fitted MXene and MoS_2, respectively. The greater number of surface-active sites in MoS_2 led to a higher removal efficiency for Cr(VI) as compared to MXene. At 298K, the highest adsorption capacities of MXene and MoS_2 for Cr(VI) were 59.805 mg/g and 113.71 mg/g, respectively. Thermodynamic investigations of both materials exhibited that the adsorption process was endothermic and spontaneous. The effect of coexisting ions was also investigated in the study that involves coexisting anions like PO_4^{3-}, HCO_3^{2-}, Cl^- and coexisting cations such as Ca^{2+}, Mg^{2+}, Na^{1+}. MXene showed a decrease in removal percentage up to 70% after fifth cycle whereas the decrease in percentage removal reached 79% in case of MoS_2 after fifth cycle. According to the findings, it can be inferred that these developed materials have the advantages of simplicity and effortless operation like adsorption for reducing heavy metal pollution.

Keywords: MXene, Molybdenum Disulphide, Water treatment, Adsorption.

CHAPTER 1: INTRODUCTION

1.1 Background of Study

The environmental damage caused by human activities has continued for years. The need for solutions to environmental issues resulting from improper waste disposal has expanded due to the expeditious development of industry and the depletion of natural resources. No doubt, water is a crucial constituent playing a notable role in all the ecosystems and has a profound impact on every facet of existence. Regretfully, the discharge of multiple contaminants, including pesticides, pharmaceutical products, and potentially hazardous metal ions, has resulted in a decline in the quality of these water resources (Abilio et al., 2021). In the earth's mantle, chromium (Cr) is one of the prevalent elements. Vaughlin made this discovery in 1797, and it is currently the 17th most abundant element in the earth's crust's mantle layer. Unlike other elements, chromium also possesses chemical and physical properties. The atomic number of chromium is reported as 24, atomic mass of 51.996 gmol^{-1}, 1.6 electronegativity. Other properties of chromium include 7.19 gcm^{-3} density, 1907 °C melting point, 2672 °C boiling point. Other literature studies report the ionic radius of chromium as 0.061 nm for trivalent chromium and 0.044 nm for hexavalent chromium and Van Der Waals radius to be 0.127 nm (Ukhurebor et al., 2021).

1.2 Prevalence of Chromium

The sources of chromium can both be natural and artificial due to human anthropogenic stresses (Peng & Guo., 2020). Increase of hexavalent chromium in the environment also occurs from the natural processes in groundwater mainly due to the interaction of existing water with ultramafic rocks (Georgaki et al., 2023). Other sources of Cr(VI) in ground water originate from geogenic sources. In these processes, natural leaching of chromium occurs into water from the surrounding rocks having higher concentrations of chromium (Boussouga et al., 2023). Additionally, Cr(VI) is formed naturally by manganese catalysis. Cr(VI) in water treatment can also result from oxidative processes such as ozonation and chlorination (Konradt et al., 2023). Numerous industries, including the tanning of leather, metal plating, electroplating, military, pigment, and refractory industries, use chromium extensively. Wastewater generated from industrial processes is a primary source of release of hexavalent chromium to water bodies mainly from cement industries, paint industries, wood preservation,

manufacturing of stainless steel, electroplating and metallurgical processes (Ojembarrena et al., 2022). Industrial effluents release chromium oxide in its +2 to +6 chemical states into aquifers and streams, among other receiving habitats. The two most recurrent forms of chromium are trivalent (CrIII) and hexavalent chromium(CrVI) owing to their malignancy and substantial impacts to the environment. The poisonousness of hexavalent chromium (CrVI) is noticeably higher than trivalent chromium (CrIII) (Ojembarrena et al., 2022). The virulency of Cr(VI) in terms of carcinogenicity and mutagenicity is 500 times greater than Cr(III) (Liu et al., 2021). Compared to the Cr(III) form, the extremely poisonous, soluble, and mobile Cr(VI) form has more detrimental effects on both people and animals (Prasad et al., 2021).

1.3 Guidelines for Hexavalent Chromium Cr(VI)

The World Health Organization has established a maximum allowable limit of 0.05 mg/L for hexavalent chromium (CrVI) in drinking water (Aslani et al., 2018). According to USEPA, permissible concentration of hexavalent chromium in water is 0.1 mg/L. These strategic standards impose the restrictions of excessive discharge of hexavalent chromium in drinking water (Ojembarrena et al., 2022). Directive drinking water of European Union recommends Cr(VI) level up to 25 µg/L (Konradt et al., 2023). Furthermore, in future, strict regulations are expected for Cr(VI) concentrations due to its potential health impacts. Hexavalent chromium is known to be carcinogenic and is the cause of numerous diseases which mainly includes lung cancer, damage to kidney and liver, gastrointestinal problems, skin and nasal irritation, eardrum damage (Heidari et al., 2021), dermatitis, respiratory disorders, and eye infections. According to international literature, hexavalent chromium is the leading cause of dysfunction of digestive system, immune system , urinary system, respiratory and reproductive systems as well (Georgaki & Charalambous., 2023).

1.4 Hexavalent Chromium Exposure

 Hexavalent chromium is also referred as Group A carcinogen (Ukhurebor et al., 2021). The effect of chromium on human body is regulated by multiple factors such as the duration of exposure, dosage of chromium intake, form of chromium which is also dependent on the route of its intake such as through food, water, inhalation or with skin contact. Hexavalent chromium exposure over an extended period of time may be harmful to health and is influenced by a number of variables, including body weight, age, and gender (Georgaki et al., 2023). Hexavalent chromium is classified in different categories depending on the time and duration

of its exposure. The exposure is considered acute if exposed to Cr(VI) for 14 days. The exposure is referred as intermediate if it lasts between 75 to 364 days and it will be chronic exposure if it extends to 365 days according to the literature reports (Yang et al., 2020; Shekhawat & Chatterjee., 2015; Georgaki & Charalambous., 2023).

1.5 Scope of Research

A great deal of researches have been completed to cure the presence of heavy metals in drinking water. Reported treatment methods for the remediation of hexavalent chromium are coagulation and flocculation, membrane separation, solvent extraction, ion exchange, reverse osmosis, chemical precipitation, electrochemical processes (Ojembarrena et al., 2022) chemical sedimentation, and adsorption techniques. However, adsorption using various materials is a growing substitute technique due to its low cost, ease of design and operation, ability to remove substances at low concentrations, low sludge generation, and environmental friendliness. The creation of a novel adsorbent with features and attributes that suggest a high adsorption capacity for metal ions is required, given the benefits of adsorption (Heidari et al., 2021). Adsorbents such as activated carbon, activated alumina, charcoal, silica gel, carbon films, clay minerals, zeolite, and biomass have all been used. Due to their lack of selectivity and weak affinity for the target heavy metals, the majority of the adsorbents listed above have limited effectiveness. Absorbency is regarded as the primary element in the adsorption of heavy metals. Choosing the best and most effective adsorption material is crucial. This kind of material needs to have a lot of surface area, lots of surface contacts, excellent adsorption sites, low cost, and a quick rate of adsorption.

MXene and Molybdenum Disulphide are regarded as two popular two-dimensional nanomaterials in water treatment. They have been investigated extensively for adsorption of environmental pollutants with numerous modifications. An emerging class of two-dimensional nanomaterials named MXenes (pronounced as maxines) was discovered in 2011 in Drexel University. MXenes is a group of two-dimensional transition metal carbides, nitrides and carbonitrides with fascinating chemical, mechanical, electrical, and magnetic properties. The general formula for MXenes nanomaterials is $M_{n+1} X_n T_x$, n ranging from 1 to 3. M in the formula represents early transition metals of periodic table such as such as Ti, Sc, W, Cr, Mo Ta, W, Zr, Nb, Hf, Y, or V), X represents carbon or nitrogen and T denotes the surface terminating group such as hydroxyl (-OH), Chlorine (-Cl), Florine (-F) or Oxygen (=O) and x

stands for the surface functionalities (Karthikeyan et al., 2021; Shahzad et al., 2019). MXenes are usually synthesized from MAX phases by selectively etching the Al atoms in layered hexagonal ternary carbide Ti_3AlC_2. On the other hand, MoS_2 is an inorganic compound which is formed by the combination of one atom of molybdenum and two atoms of sulfur, and it is categorized as transition metal dichalcogenides (Ali et al., 2022). MoS_2 nanosheets can be synthesized by numerous techniques. Some of the methods reported in the literature are chemical vapor deposition, chemical exfoliation, mechanical exfoliation, electrochemical exfoliation, liquid exfoliation, and hydrothermal synthesis.

The aim of this study is to compare the performance of two-dimensional MXene and MoS_2 in unmodified form for the removal of hexavalent chromium under identical working conditions. MXene was synthesized by the process of etching. Room temperature is more suitable for the etching process due to the exothermic reaction. For this purpose, Ti_3AlC_2 was etched using ammonium (NH_4F) as an etching agent. The reaction was completed after 24 hours to successfully synthesize $Ti_3C_2T_x$ MXene. Hydrothermal synthesis was opted for synthesis of MoS_2 with increased surface area. Materials were synthesized and tested through different characterization methods. XRD, FTIR, SEM, EDS and BET surface area analysis were performed to depict the crystallinity of the adsorbents, investigation of the functional groups, morphology of structures and their elemental composition, and to check the surface area of MXene and MoS_2, respectively. Adsorption studies were conducted to investigate the use of efficient two-dimensional nanomaterials for Cr(VI) removal. Furthermore, the adsorption capacities of MXene and MoS_2 were compared for Cr(VI) adsorption.

1.6 Aims and Objectives

1.6.1 Aim

The aim of this study is to compare the performance of two-dimensional MXene and MoS_2 in unmodified form for the removal of hexavalent chromium under identical working conditions.

1.6.2 Objectives

1. Synthesis of MXene and MoS_2 by etching and hydrothermal method, respectively.

2. Characterization analyses of both materials through XRD, SEM, EDX and FTIR analysis.

3. Study of various adsorption parameters for the adsorption of Cr(VI) using MXene and MoS$_2$.

4. To assess the impact of regeneration studies on the performance of adsorbents for Cr(VI) removal.

CHAPTER 2: LITERATURE REVIEW

2.1 Importance of Water

Since water is thought to be the most plentiful and vital resource for life on Earth, water pollution has become a major global concern. Rising population, fast industrialization, and changing consumption habits caused the world's water consumption to increase by a factor of six between 1900 and the current decade. Consumption is increasing at a rate of 1 % per year, which should alert humanity to the need to protect its water supplies (Mohanapriya et al., 2023). One essential natural resource for the continuation of life is water. Ten countries in Southeast Asia and the Pacific region rely on groundwater as one of their major domestic resources. About 66 % of urban households and 60 % of rural households rely on this for their drinking needs. Furthermore, it is estimated that by 2050, the global demand for freshwater would rise by up to 70 %. Even still, just 0.76 % of the world's water resources are fit to drink. Programs to protect water resources should therefore be put into place in several nations. Population outburst and industrialization have increased fresh water demand and incurred a stress on water bodies and maritime habitat due to rapid excretion of pernicious heavy metals and chemical pollutants in to the water bodies (Zhao et al., 2019). In fact, 2 million tons of wastewater is estimated to mix with natural water systems daily (Geissen et al., 2015; Geng et al., 2019). Unfortunately, in developing countries, 90 % of the sewage water is released in water bodies without treatment (Hairom et al., 2021), and 300 to 400 megatons of industrial waste is dumped into water bodies annually (Boretti & Rosa., 2019). Wastewater generated from industries alone contributes to 16 % of the world's generation of wastewater (Younas et al., 2022). The deterioration of natural water system due to heavy metals, such as mercury, lead, chromium, and arsenic is a major global environmental concern (Ledezma et al., 2021).

2.2 Heavy Metals

Heavy metals are poisonous and accumulate in water bodies. Due to their toxicity, they pose the biggest threat to the ecological balance. Heavy metals are gathered in the aquatic ecosystem through man-made or natural channels. The addition of heavy metals resulting from natural occurrences such soil erosion, volcanic eruptions, and aquatic life metabolism does not impact the food chain or ecological balance. On contrary, the aquatic ecology is heavily impacted by the man-made heavy metals discharged from cities, industries, and agriculture (Mohanapriya

et al., 2023). With densities over 5 g/cm^{-3}, heavy metals are inorganic pollutants that pose a concern to the ecosystem and human health because of their everlasting nature and bioaccumulation, which also results in their carcinogenic and mutagenic properties (Ramli et al., 2023). Different types of chromium (Cr) exist in nature depending on its oxidative states. One of the most prevalent heavy metals in the environment is hexavalent chromium Cr(VI), a hazardous metal ion that has been demonstrated to be 1000 times more harmful than trivalent chromium Cr(III).

2.3 Toxicity of Chromium

On its Substance Priority List, the US Environmental Protection Agency places Cr in 17th position, reflecting its higher danger level in comparison to other compounds (Ahmad et al., 2019). In order to handle these compounds safely, authorities have also developed a number of safety protocols. For example, the Occupational Safety and Health Act and the National Institute of Occupational Safety and Health have established the maximum permissible levels of Cr for mercury vapor exposure at 0.05 mg/m^3 and 0.0002 mg/m^3, respectively, in the workplace. The World Health Organization established a tolerable limit of 0.05 mg/L for Cr in drinking water (Ramli et al., 2023). Chromium is contemplated as the 21st most occurring element present on the Earth's surface. The natural presence of hexavalent chromium is (0.2 - 1 µg/L) in rainwater (0.04-0.51 µg/L) in sea water, (0.5-21 µg/L) in surface water and <1 µg/L in ground water (Vaiopoulou & Gikas., 2020). The US Environmental Protection Agency's (EPA) allows maximum limit for chromium in drinking water to be <0.1 mg L^{-1}, while World Health Organization's is 0.05 mgL^{-1} (Jin et al., 2019; Vilela et al., 2019). Chromium is considered as the 129th concerned contaminant and is ranked as the 14th most polluting heavy metal by (EPA) Environmental Protection Agency (Sharma et al., 2012). In industrial wastewater, the concentration of chromium ranges from 0.5 to 270000 mg/L (Kumar & Dwivedi., 2021). Topmost countries in the chromium mining industries include South Africa, China, India, and Kazakhstan (Lukina et al., 2016).

2.4 Sources of Chromium

Anthropogenic sources of chromium include leather tanning, electroplating, aerospace, alloys, metal ceramics, metal finishing, chromate production, paint and pigments, dye paints, wood preservation, manufacturing of synthetic rubies, and steel manufacturing industries (Almeida et al., 2019). The trivalent chromium species Cr(III) exists predominantly in the natural

systems, while the hexavalent species Cr(VI) is the second most stable form originated mainly from industrial sources (Hiller & Leggett., 2020). Although Cr(III) is extremely important for lipid and sugar metabolism and is consumed by humans as dietary supplements, it has a lower solubility and bioaccumulation potential than the Cr(VI), which has harmful health effects (Periyasamy & Viswanathan., 2018), including diarrhea, kidney and liver damage, hemorrhaging, gastric damage, vomiting, nausea, and lung cancer (Anirudhan & Senan., 2011) (Karthikeyan et al., 2020). Sources of chromium from industries include wastewater from leather tanning, ceramic glazes, lumber modification, wood preservation, electroplating, textile wastewater, dyes from clothing industries, mordants, paints and pigments, pulp and paper production, alloying, industrial cooling towers, refractory bricks, metallurgy, and road dust.

2.5 Health Impacts

Numerous waterborne illnesses, including skin allergies, kidney failure, circulatory problems, gastrointestinal distress, cancer, blue baby syndrome, nervous system disorders, and bone weakness, are brought on by contaminated water. It is estimated that 53,000 children perish from various waterborne illnesses each year, primarily from diarrhea (Adewumi., 2022; Fida et al., 2023). Numerous occupational studies on workers who were exposed to chromium (VI) dust or vapor on a long-term basis have documented effects on the respiratory system, such as dermatitis, bronchitis, reduced lung function, itching, rhinorrhea, sneezing, nose bleeding, ulcerations and perforations, and bronchitis. Asthma may also have been noted in certain instances. Lung cancer and other adverse consequences, including liver and kidney failure, nasal inflammation, allergies, and burning in the lungs, have been linked to exposure to Cr(VI) (Ramli et al., 2023). Additional research on humans showed that long-term exposure to Cr(VI) in drinking water may raise the risk of prostate, bladder, kidney, and stomach cancers. In addition, it may result in aberrant hematological function, gastrointestinal disorders, dermatological problems, and hypertension in expectant mothers. Cr(VI) in the body at a low quantity (0.1 mg/g) has the potential to be fatal (Astuti et al., 2023).

2.6 National Scenarios

Pakistan's drinking water quality is gradually declining as a result of the country's worrisome population increase, fast industrialization, changing climate, and ineffective water quality management. Most people in Pakistan are compelled to consume contaminated water since they lack access to sources of clean, safe drinking water. Water bodies around the world may

have increased Cr (VI) concentrations following the release of untreated wastewater containing Cr from the steel and metal processing industries, electroplating, and leather tanning processes. In light of this, there are clearly highly contaminated sites with Cr (VI) in Pakistan's industrial areas, with levels of the metal surpassing safe limits in soil (6900–19,500 mg/kg) and drinking water reservoirs (1.990–13.53 mg/L) (Usmani et al., 2023). Vredenburg found a vast supply of chromite in the Muslim Bagh area of the Qila Saifullah district of Baluchistan province, Pakistan, in 1901. The chromite reserves in the Muslim Bagh valley, a well-known chromite hub of the nation, cover an area of around 2000 km. The country's economy greatly benefits from the chromium mining operations in this region, but the environment and local population are also seriously threatened, and major health problems are brought on by these activities (Chandio et al., 2021). In order to evaluate the level of heavy metal contamination in Malakand Agency, 75 water samples were taken from hand pumps, springs, tube wells, dug wells, and bore wells. The allowable limits of the World Health Organization and National Standards for Drinking Water Quality were surpassed by the heavy metals, including Cd (12 mg/L), Ni (77mg/L), Cr (61 mg/L), Mn (78(mg/L) and Pb (16 mg/L) (Nawab et al., 2016; Fida et al., 2023). The large contribution to leather exports came from a number of manufacturing units concentrated around Korangi, Karachi. Aside from the unofficial count, which is far more than the above total, there are approximately 170 tanneries documented in Korangi, Karachi. Thus, Korangi tanneries are well-known and noted for their detrimental effects on the environment and pollution levels, especially when it comes to chromium. Selective parameters (total suspended solids, total dissolved solids, pH, biochemical oxygen demand, chemical oxygen demand, and chromium) were analyzed, and the findings were found to be within permissible limits (in April, May, and June) with the exception of chromium, which had values that exceeded 10.26 mg/L and 13.05 mg/L in May and June, respectively. The permissible limits of hexavalent chromium by Sindh Environmental Protection Agency is < 1mg/L. The analysis's findings highlighted the need for effective tanning procedures, optimum industrial practices, chromium recovery, and recycling (Neelam., 2018). The primary industry that consumes chromium is the tanning sector. Although there are tanning industries all throughout Pakistan, Sialkot, a tiny industrial city, has the highest concentration of tanning industries. Wastewater samples were gathered from various tanneries and Nullah Aik, located in Sialkot, and subjected to analysis in order to determine the pollution level. The effluent sample showed high levels of total solids (2265-19314 mg/L), total dissolved solids (1313-17467 mg/L), hexavalent chromium (1.8-9.8 mg/L), total chromium (3.75-16.7 mg/L), pH (5.1-10.9), biological oxygen

demand (335-5818 mg/L), and chemical oxygen demand (740-14546 mg/L) (Riaz & Zia., 2020). Another study was conducted for the investigation of total chromium and hexavalent chromium in Sheikhupura and Kasur cities of Pakistan and the results demonstrate that Comparable Cr(VI) level was found in the wastewater of the Sheikhupura and Kasur tanneries at head, but significantly greater total Cr (in parentheses) was found subsequently, at 89.7 mg/L (1440.57 mg/L) and 94.9 mg/L (3527.95 mg/L). The Cr(VI) level decreased as one moved farther down the stream, decreasing steeply at Kasur and exponentially at Sheikhupura (Benjamin & Nishat., 2021). High levels of chromium were also shown in multiple studies conducted by (Shakil et al., 2023; Younas et al., 2023) and the results were exceeding the permissible limits.

2.7 International Scenarios

A study conducted in the Sukinda Valley of India shows high levels of hexavalent chromium as India is listed as the world's third supplier of chromite. According to a May 2021 scientific study, the Sukinda region's overall atmospheric chromium concentration ranges from 10 to 400 mg/L (parts per million), much beyond the permitted limit of 0.1 mg/L. Surface water and groundwater have been found to have 3.4 mg/L and 0.6 mg/L of chromium(VI) contamination, respectively, while the safe threshold of 0.05 mg/L remains unsurpassed. The safe assumable limit of 0.05 mg/L for hexavalent chromium has been significantly exceeded by the quantity of the metal in the mining water. Mining water contamination (0.01–4.25 mg/L) surpasses both surface water (0.03–0.56 mg/L) and groundwater (0.01–0.59 mg/L), despite their higher counts. Hexavalent chromium was found to be more contaminated in the mining water than other Cr-species, whereas both surface and groundwater samples had large amounts of chromium(III). As a result, the deposition of heavy metals like chromium has led to an increase in toxicity in water bodies (Mohanty et al., 2023). A study conducted in Bangladesh for determining the toxic effects of dam's construction in tannery effluent with high chromium concentration demonstrated that for the obstruction construction period, the mean concentration of Cr(VI) in the upstream canal water was 52.1 μg/L, which was greater than the downstream canal water's 1.36 μg/L concentration for the same period. During the barrier erected period, nearly 50% of the upstream canal water samples had Cr(VI) concentrations above the US-EPA's Cr(VI) guideline threshold of 16 μg/L. Even during the time when there were as many tanneries as possible prior to the relocation of tanneries (the nonblockage period), the proportion of canal water samples with Cr(VI) concentrations over the recommended level

was just 4-5 percent. These findings suggest that the isolation of upstream and downstream canal water by the blocking construction caused an unexpected increase in Cr(VI) pollution (Kurniasari et al., 2024). Another study conducted in Chinese Loess Plateau to determine the Concentration of hexavalent chromium in four different rivers named as Bali river, Luo river, Xingzi river and Wuding rivers. The Cr(VI) values throughout the region varied from 0.005 to 0.251 mg/L, with a mean of 0.049 mg/L (He & Li., 2020).

2.8 Techniques for Cr(VI) Removal

Chemical precipitation, ion-exchange resin , coagulation, reverse osmosis, membrane filtering, electrodialysis, electrochemical treatment, photocatalysis, biological treatment , and adsorption are among the different methods established for Cr(VI) removal.

2.8.1 Chemical Precipitation

Because of its low operating costs and convenience of use, chemical precipitation is widely used in industrial processes. Heavy metal ions are precipitated by the precipitating agents as insoluble precipitates that are easily separated by sedimentation or filtering during precipitation. Reusing the purified water is possible. Precipitation based on sulfide and sodium hydroxide is typically used in chemical methods. Chemical precipitation was the method Ramakrishnaiah and Prathima (Prokkola et al., 2020) tried to remove Cr (VI) from industrial effluents. Studies conducted in laboratories using sodium hydroxide, iron chloride and calcium hydroxide as precipitants range. A sludge production of roughly 7 ml/L was found, indicating a 99.7 % removal effectiveness of Cr (VI). The authors draw the conclusion that sodium hydroxide and calcium hydroxide are appropriate precipitants for the elimination of chromium (Kerur et al., 2020).

2.8.2 Coagulation/Flocculation

The methods of flocculation and coagulation are employed to extract suspended particles from the effluents. Particle size, shape, and density all affect how well suspended particles separate. Similar surface charges on suspended materials resist one another, keeping them suspended in water. Through sedimentation, flocculation and coagulation increase collision of particles, counteract changes on surface, and expand floc. Coagulants produce micro flocs, which are tiny, suspended particles, by counteracting the negative surface charges found on non-settleable materials. Collisions of particles and proper coagulation are encouraged by agitation, which

11

also disperses the coagulant. Usually, the rapid-mix chamber has a contact time of one to three minutes. Particle size is increased by flocculation, resulting in larger flocs known as pin flocs from micro flocs. The duration of flocculation contact is 15 to 20 minutes. To avoid tearing apart flocs, the mixing velocity is gradually reduced. Low soluble chemicals such as hydroxides, sulfides, and carbonates are precipitated using coagulation procedures (Ghernaout., 2015). A suspension of atoms or molecules with a density equivalent to that of water is called a colloid. The low density prevents these particles from settling. These colloidal particles are eliminated, and the density is increased via the coagulation treatment process. The kind of coagulant, dosage, temperature, alkalinity, pH, and mixing conditions all affect coagulation efficiency. Chemical reagents, also known as inorganic flocculants, such as $Al_2(SO_4)_3$, $Fe_2(SO_4)_3$, and $FeCl_3$, as well as its derivatives, such as poly aluminum chloride and poly ferric chloride, are utilized in this approach of treating wastewater (Kerur et al., 2020).

2.8.3 Ion-Exchange

Ketonic granular particles with a chemical structure that encourages the exchange of basic or acidic radicals are known as ion exchange resins. The ions of the same signs that are present in the solution in contact with these radicals replace the positive or negative ions that are present on their surface. In the ion exchange process, sludge generation proceeds somewhat slowly. Anion and cation exchange resins are part of an ion exchange system. Anionic resins are appropriate for wastewaters with low concentrations. Ion exchange was employed to treat Cr (VI) and Mn (II). The ion exchange method has drawbacks that restrict its application for treating industrial wastewater, including the need for chemical reagents to regenerate the ion exchange resin, the production of a lot of backwashing water, and high operating costs (Kerur et al., 2020).

2.8.4 Reverse Osmosis

Based on the principles of charge exclusion and size exclusion, reverse osmosis (RO) selectively eliminates dissolved contaminants using a membrane that is either semi-permeable or selectively permeable and has a thickness ranging from 0.1 to 1.0 nm. Only water molecules are allowed to pass through desalination plants. Applications of RO for heavy metal removal in wastewater treatment are growing. (Petrinic et al., 2015) investigated the removal of suspended particles and heavy metal ions from industrial effluents by combining ultrafiltration with effluent treatment from the metal finishing industry.

2.8.5 Adsorption

Adsorption is defined as a process that involves the deposition of a substance or pollutant on the adsorbent's surface at higher concentration in molecular form. The process of adsorption depends on the layer of adsorbent having unique surface structure that can capture micro pollutants on its surface. This process is effective due to lower energy consumptions and the ability of available raw materials to capture the heavy metals even at lower concentrations. Two common types of adsorption are known as physisorption and chemisorption. In case of sorption the interaction between adsorbent and adsorbate takes place due to the van der Waals forces whereas in chemisorption adsorbate is attached on the surface of adsorbent by forming chemical bonds (Maftouh et al., 2023).

Adsorption is expressed by the following equation (Kerur et al., 2020).

$$q_t = (C_o - C_e) * V) / m \tag{1.1}$$

Where m represents the mass of the adsorbent, C_o and C_t represent the initial and final concentrations of adsorbate at time t, V is volume, and the q_t is adsorption capacity at time t.

2.9 Nanomaterials

In literature, four major types of nanomaterials are identified. These are zero-dimensional (0D), one-dimensional (1D), two dimensional (2D), and three-dimensional (3D) on the basis of nanoscale dimensionality principle as shown in Figure 2.1 (Khan & Malik., 2019). 2D-layered nanomaterials have garnered huge interest in both industry and science because of their applications in electronic devices, catalysis, sensing, hydrogen evolution, air purification, batteries, fuel cells, and water treatment due to their remarkable characteristics (Santhosh et al., 2016). Two dimensional nano adsorbents are extensively studied and utilized for reducing the toxicity of heavy metals from water (Ihsanullah., 2020; Peng et al., 2017; Xu et al., 2018; Liu et al., 2019; Tran et al., 2019; Liu et al., 2019; Peng et al., 2017).
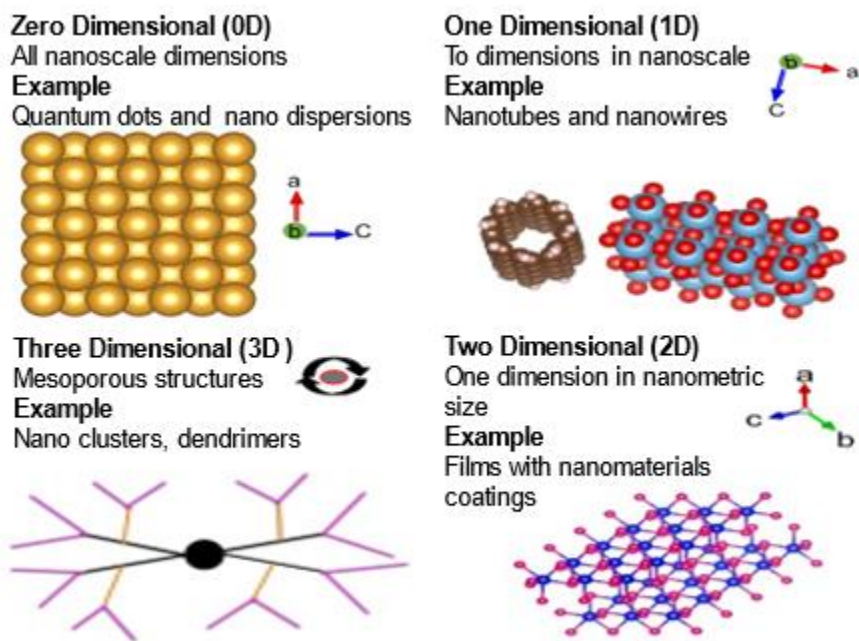
Figure 2.1: Types of nanomaterials

Presently, the technologies for chromium remediation include precipitation, electrocoagulation, nanofiltration, reverse osmosis, membrane processes, bioremediation, catalytic transformation, and adsorption. Among the available technologies, adsorption is an effective, less expensive, and sustainable option for eliminating contaminants from drinking water (Karthikeyan et al., 2020). Several materials are being modified to be used as adsorbents such as saw dust, wheat straw, coconut husks, and food waste (Salleh et al., 2011). The aim of using these materials is to control waste by utilizing them in water treatment by adsorption. However, these natural materials often show poor selectivity and low adsorption efficiency, arduous efforts were made to develop and use industrial adsorbents, such as carbon nanotubes, silica, activated carbon and zeolites to achieve better performance.

2.9.1 Emerging Nanomaterials

The requirement for nanoscale material becomes critical. Because of the exceptional qualities that come with being so small, nanomaterials have gained popularity and show great promise as trustworthy adsorbents for the effective removal of heavy metals from the environment. Many kinds of nanoparticles, including polymeric nanocomposites, quantum dots, carbon-based nanomaterials, metal oxide nanoparticles and clay nanocomposites, have been studied for their potential as nano adsorbents for the treatment of heavy metals. Their huge surface area

and small size make them effective adsorbents for cleaning up different types of environmental pollutants (Inobeme et al., 2023). Some of the nanomaterials are discussed in detail.

2.9.1.1 Graphene based nanomaterials.

Graphene belong to two dimensional nanomaterials, and it is composed of sp_2 hybridized carbon atoms arranged in a strong hexagonal lattice. Its unique structure makes it impervious to all other atoms and molecules, having high surface area of 2630 m^2/g (Aigbe & Osibote., 2020), high thermal conductivity up to 3000 W/mK. Young's modulus of graphene is shown to be 1060 GPa. Due to its two-dimensional nature and unique layer arrangement of atoms, graphene has shown exceptional performance in various applications. In addition to that, Graphene Oxide (GO) is a two-dimensional material with micron-sized dimensions and multiple active oxygen and hydroxyl groups on its surface, making it an ideal substrate to support a variety of nanoparticles (Yu et al., 2018). GO has gained attention for separation of heavy metals from water because of its excellent stability, hydrophilic nature, and adsorption capacity (Ahmad et al., 2020). The remarkable adsorption performance of GO is attributed to multiple oxygenated functional groups (e.g., carbonyl, carboxyl and hydroxyl) on its surface (White et al., 2018). To further improve the heavy metal removal capability of GO, chemical functionalization is applied on graphene made through Hummers methods. Acid treatment is applied on graphene oxide to transform it to graphene nanosheets before functionalization, which is the process of modifying the surface properties of the material by incorporating new functional groups via adsorption or chemical bonding. Both covalent and noncovalent alteration methods are utilized in the functionalization of graphene. The resulting functionalized graphene will allow the faster removal of heavy metals than other nano materials.

2.9.1.2 MXene based nanomaterials

MXenes, being a class of two-dimensional nanomaterials, are used in various environmental remediation practices such as catalysis, energy storage and water treatment. MXenes are used as adsorbents in water treatment because of their exceptional surface characteristics, including excellent surface functionalization, greater hydrophilicity, and enhanced chemical stability. MXene are represented by the generic formula written as $M_{n+1} X_n T_x$, in which M is expressed as an early transition metals e.g., W, Ti, Zr, Mo etc., X signifies nitrogen/carbon, T signifies termination groups on surface such as chlorides or fluorides and x stands for distinct functional

groups and value of n can be in between 1 and 4. Chemical etching of A layers from the parent MAX phases is typically applied to synthesize MXenes. Different protocols are adopted to improve the performance of MXenes for metal adsorption applications. The negatively charged MXene sheets produced via wet chemical etching usually have abundant (OH, O, F and Cl) functional groups, making them suitable for collecting positive heavy metal ions including hexavalent chromium. MXene is usually synthesized through etching and delamination from MAX phase (Alhabeb et al., 2017) and . Figure 2.2A discussed the delamination of single layer MXene with improved intercalation through etching followed by delamination.

MXenes have shown exceptional performance in a variety of applications due to their remarkable structural characteristics. They possess various metallic hydroxide sites that are easy to functionalize due to greater specific area, broader interlayer spacing and increased chemical stability. Preventing water bodies from being contaminated by toxic heavy metal ions is critical to safeguard living organisms and aquatic life. Therefore, MXene-based nanomaterials are being explored for eradication of heavy metal ions from drinking water in multiple research studies by adsorption. In a study (Wang et al., 2020), it was reported that reduction and adsorption of hexavalent chromium can be enhanced by increasing the active sites and surface area of adsorbent. Ti_3C_2/TiO_2 composite is fruitful in the confiscation of Cr(VI) as compared to pure Ti_3C_2/TiO_2 nano sheets as shown in Figure 2.2B due to the unique structure and properties of MXenes, they offer numerous adsorption sites and effective elimination of heavy metals from water such as lead, mercury, chromium barium etc.

To increase the practical applicability of MXenes in adsorption of heavy metals, regeneration of MXenes is paramount. Literature reports different solutions that have been effectively used in the adsorption process. Two common solutions reported in the regeneration of chromium are HCl and NaOH. The use of regeneration solution depends on the targeted pollutant, whether it is cationic or anionic pollutant, due to varying adsorption mechanism (Karthikeyan et al., 2021; Sheth et al., 2022). The cationic heavy metal ions are generally adsorbed in acidic medium through electrostatic repulsion mechanism in adsorption process dependent on pH (Chai et al., 2021). HCl is mostly used for the regeneration of positively charged pollutants such as Pb, Hg and NaOH is used in regeneration of anionic pollutant species such as arsenic and Cr(VI) (Sheth et al., 2022).
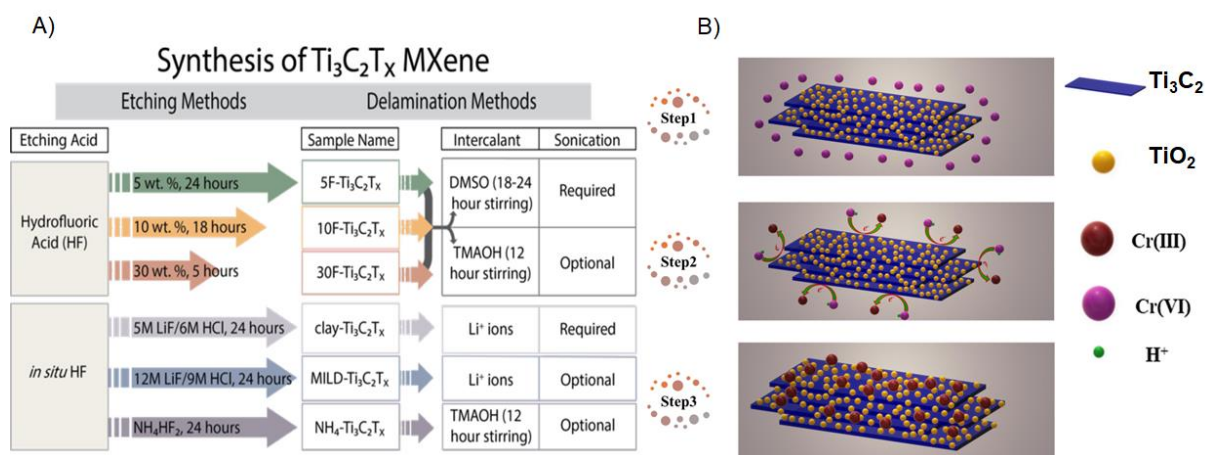
Figure 2.2: (A) MXene synthesis from MAX phase (Alhabeb et al., 2017). (B) A schematic description for the removal of hexavalent chromium by Ti_3C_2/TiO_2 composites (Wang et al., 2020).

2.9.1.3 Molybdenum disulfide-based nanomaterials

Molybdenum disulfide consists of two layers of sulfur atoms sandwiching a layer of molybdenum atom. The strong covalent bonds hold the Molybdenum and Sulfur atoms together while the atomic layers of Sulfur-Molybdenum-Sulfur are linked to each other by van der Waals interaction forces. These weak interaction are easily broken, and infiltration of other molecules or ions into the layers of MoS_2 becomes easy. MoS_2 forms two-dimensional shapes because of its anisotropic structure Figure 2.3A which makes it a suitable candidate for adsorption of heavy metal ions because of its permeable channels and greater surface area. In addition to surface area many other factors such as its thermal and chemical stability, hydrophilicity, excess sulfur groups on its surfaces, excellent dispersibility and edges make MoS_2 a good adsorbent for heavy metal ions (Sun et al., 2018). Each layer of MoS_2 is almost 0.62 nm thick and the interlayer distance in each layer is almost 0.30 nm. MoS_2 is capable of adsorbing heavy metal ions through three mechanisms: electrostatic interaction, redox reaction, and complexation. Due to its strong binding affinity with heavy metals, S ions can form S-heavy metal complexes on the surface of MoS_2 and makes the removal of Cr(VI) ions faster from water bodies (Liu et al., 2019). Additionally, the negatively charged MoS_2 adhere to positively charged pollutant ions through electrostatic interaction. Adsorption due to electrostatic interactions may not be much significant as compared to sulfur chemical complexation as the charge distribution on the surface of MoS_2 changes once the inner layers of MoS_2 undergo complexation with cations. While electrostatic interactions may not be as

17

significant as chemical complexation, they are advantageous for removing heavy metal ions that do not have an affinity to bind with MoS_2 through complexation, such as cobalt and copper ions (Liu et al., 2019).

Another possible mechanism for adsorption of hexavalent chromium ions on MoS_2 surface is by redox reaction. Redox reaction mechanism is only suitable for some heavy metals, which is attributed to their redox potentials. Heavy metals having higher redox potential than SO_4^{2-}/MoS_2 and MoO_4^{2-} pair (0.429 V) potential (Zhu, et al., 2016; Bussche, et al., 2016) can only be adsorbed by two dimensional MoS_2. This is the only case which permits the elimination of pollutants by MoS_2. If the redox potential is less than 0.429 V, then the confiscation of heavy metals by adsorption process on MoS_2 is achieved either by electrostatic interaction or though chemical complexation. As shown in the Figure 2.3B (Cai et al., 2020) reported that redox potential of CrO_4^{2-}/Cr^{3+} pair (1.35eV) is higher than MoO_4^{2-}/MoS_2 pair (0.429 V) which allowed MoS_2 to reduce chromium (VI) ions (Wang et al., 2018; Bussche, et al., 2016). The higher redox potential confirms that a redox reaction occurred between CrO_4^{2-} species and $MoS_2/CTAB$ in addition to adsorption.
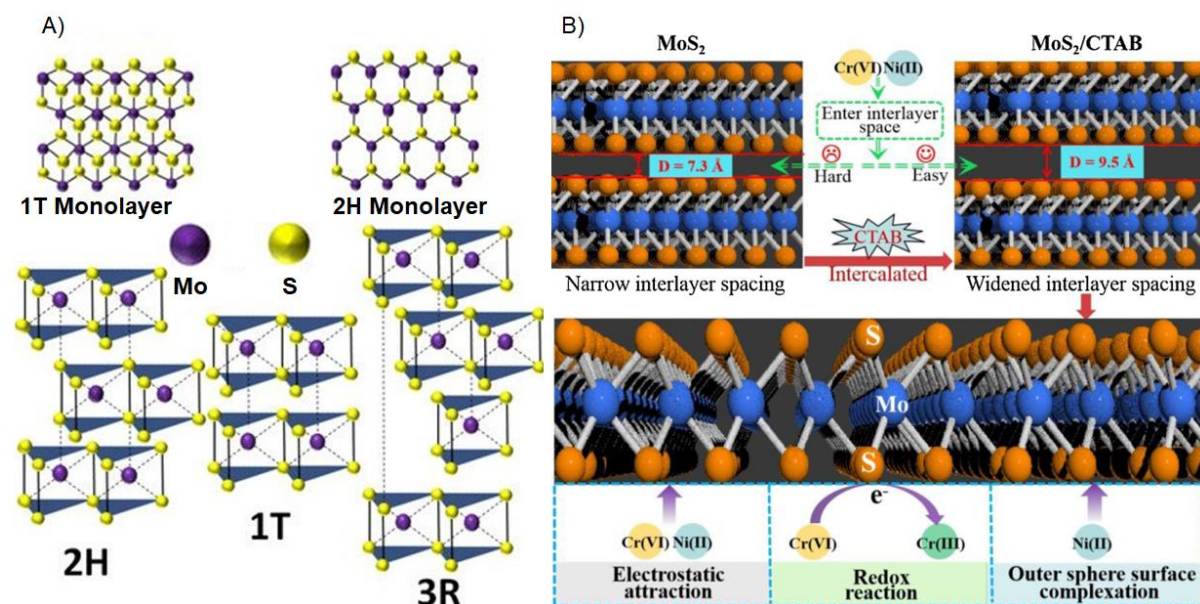
Figure 2.3: Top view of 2H/1T MoS_2 monolayer and polymorphic structures of MoS_2 (Mouloua et al., 2021). (B) Elimination of Cr(VI) and Ni(II) ions by CTAB–intercalated MoS_2 nanosheets (Cai et al., 2020).

2.10 Key Influencing Parameters for Cr(VI) Adsorption

2.10.1 pH Effect

The treatment of hexavalent chromium is highly pH dependent as it can change the structure of adsorbate, functionality on the surface of adsorbate, speciation of ions, the dissociation of termination groups and degree of ionization in water solutions (Ahmed et al., 2021).The speciation of hexavalent chromium is highly pH dependent. At lower pH values below 7, the existing species of Cr(VI) reported are H_2CrO_4, $HCrO_4^-$, CrO_4^{2-} and $Cr_2O_7^{2-}$. The higher adsorption of chromium is reported at pH 1 and pH 2 where the species of chromium exist as H_2CrO_4, and $HCrO_4^{-,}$ respectively (Avila et al., 2014). Therefore, pH is counted as a significant factor in the adsorption process of heavy metal ions. Chromium (VI) adsorption by synthesizing green silicon nanoparticles conducted at the specific dose of 100 mg/L for 60 min keeping the initial concentration 50 mg/L with pH of solution between 2 to 7 and the highest removal percentage achieved at pH 4 (Mehmood et al., 2022). Chromium exists as $HCrO_4^-$, H_2CrO_4, and $Cr_2O_7^{2-}$ in the pH range 3 to 6 (Yao et al., 2020), whereas the ions of chromium existing in the pH range of 6 to 12 are mostly reported as $Cr_2O_7^{2-}$ (Zhang et al., 2019) which are difficult to reduce in comparison to other chromium ions (Kekes et al., 2021). Acidic pH range is more favorable for the adsorption of chromium ions as compared to alkaline pH due to the excess of positive hydronium ions which attracts the negative ions (Mehmood et al., 2022). Similar results are shown for adsorption of chromium into polyimidazoles chain attached to surface of MXene (Ti_3C_2@Imidazoles) in which highest removal was seen at pH 2 and further increases in pH resulted in reduced adsorption capacity (Yang et al., 2021). Adsorption of chromium ions is also confirmed by reduced graphene oxide hydroxyapatite composite in which the highest adsorption capacity of 45.24 mg/g was attained at pH 2 attributed to the strong attraction between positive adsorbent surface and negative chromium ions (Karthikeyan et al., 2021). In the case of MoS_2, chromium removal is also achieved maximum at acidic pH. The results are confirmed by a study performed by (Xiang et al., 2021) indicating the impact of pH on chromium adsorption over a wide range from 2 to 10. Polypyrrole / MoS_2 showed highest hexavalent chromium removal a pH 2 as compared to MoS_2 and Polypyrrole. $HCrO_4^-$ and $Cr_2O_7^{2-}$ chromium species were dominant at pH value ranging from 2 to 6. The surface performance of the samples eliminated most of the Cr(VI) species at lower pH. Electrostatic sorption capacity of different adsorbents can be determined through zeta potential. The calculated pH_{pzc} of Polypyrrole and Polypyrrole/MoS_2 in this study are

reported to be 7.9 and 7.5 respectively. $pH_{pzc} > pH$ indicates the positive zeta potential showing the excess of H^+ ions which speeds up the removal of Cr(VI) through electrostatic attractions. And when the $pH > pH_{pzc}$, the elimination of Cr(VI) reduces due to repulsive forces (Xiang et al., 2021).

2.10.2 Dosage Effect

The investigation of impact of adsorbent dosage on adsorption of heavy metal ions is investigated in multiple researches. Dosage of adsorbent directly impacts the efficiency and capacity of adsorption. It is also dependent on the economy of the process so the choice of optimum dosage for improved adsorption is quite essential (Khurshid et al., 2022). The adsorption capacity varies with change in dosage of the adsorbent. For example, a study completed by (Singh et al., 2022) reported that dosage increase of adsorbent from 1 g/L to 5 g/L resulted in the improved removal efficiency of hexavalent chromium from 41.5 to 96.05 % at an initial Cr(VI) concentration 5 mg/L with pH of solution 8.02 However, the results did not show high percentage removal when the dosage increased above 2 g/L as demonstrated in. Adsorbent dosage improves the removal efficiency up to a certain limit and it is attributed mostly to the number of increased adsorption sites. As the adsorption sites are saturated then further increase in the dosage does not show positive impact in the removal of pollutant (Lyu et al., 2017; Zhang et al., 2019). Effect of adsorbent dosage on Cr(VI) adsorption by the MXene-chitosan (Wan et al., 2021) is depicted in which the increase in the dosage of adsorbent from 0.02 to 0.12 g/L resulted in increased removal efficiency from 12.9 % to 40.5 % due to more contact surface and availability of greater number of adsorption sites. However, the adsorption capacity kept declining from 30.5 mg/g to 16.1 mg/g because limited amount of hexavalent chromium can be adsorbed or removed by the adsorbent.

2.10.3 Temperature and Time Effect

Adsorption experiments have been widely performed on the removal of chromium at room temperature, which typically ranges from 20 °C to 30 °C (Almeida et al., 2019). This temperature range is generally considered cost effective as there is no need for expensive heating and cooling solutions. As the temperature increases up to 45 °C, the adsorption reactions become generally endothermic (Tang et al., 2021). Recent studies by (Wang et al., 2022) indicate maximum adsorption capacity is achieved at highest value of temperature, which suggests that the reaction is endothermic.

Emerging nanomaterials usually perform the process of adsorption within minutes and are further modified to make the process faster. The adsorption capacity of chromium varies significantly with changes in contact time. In general, the increasing time of adsorption enhances the adsorption initially and as time passes it slows down until the equilibrium is achieved. The sudden decline in the percentage removal is due to more availability of active adsorption sites at the beginning of the experiment which keeps reducing with passing time. Similar results are shown in the study conducted by (Jiang et al., 2017), demonstrating the influence of contact time on the adsorption capacity of chromium at three different concentration, 30, 50 and 70 mg/L, respectively.

2.10.4 Concentration Effect

The adsorption capacity of two-dimensional nanomaterials raises with an increase in initial concentrations of the chromium solutions. Results can be confirmed from the multiple researches (Harijan & Chandra., 2016; Tang et al., 2021) showing the similar trends for change in adsorption capacity with increasing initial concentrations. Results have shown a decline in `percentage removal with an increase in concentration while the adsorption capacity raises by increasing initial chromium concentrations. Another study completed by (Wang et al., 2022) confirms that the adsorption capacity of Cr(VI) increases until the adsorption limit of the adsorbent is achieved. The trend increases with change in initial concentration from 300 to 550 mg/L with decreased removal efficiency of hexavalent chromium.

CHAPTER 3: METHODOLOGY

3.1 Chemical Reagents

Ternary carbide MAX powder (Ti_3AlC_2) was purchased from Dr. Asif Shahzad (Uppsala University, Sweden). Hydrochloric acid (49%), Ammonium Fluoride, Polyvinyl Pyrrolidone (PVP), Sodium Hydroxide, Potassium Dichromate, Syringe Filters, Acetone, Diphenyl Carbazide (DPC), Orthophosphoric Acid, Thiourea, Ammonium Heptamolybdate, Acetic Acid Tetrahydrate, Ethanol was purchased from Sigma Aldrich. All necessary chemicals were utilized without any additional purification. For experiments and washing, deionized water was used.

3.2 Synthesis of MoS₂

For the preparation of MoS_2, 5 mmol of ammonium heptamolybdate ($(NH_4)_6Mo_7O_{24}$) was dissolved in 25 mL of water at 25 °C. 0.15 g of polyvinyl pyrrolidone (PVP) K30 ($(C_6H_9NO)_n$) was added to the mixture at low temperature using an ice bath. The solution was further sonicated for 60 minutes. After sonication, 10 mmol of thiourea (CH_4N_2S) was immersed in the solution and continuously stirred for 30 minutes. A further 1.5 mL of acetic acid (CH_3COOH) was added to the solution before transferring the solution to autoclave. The autoclave was kept in a 180 °C oven for a whole day. After the autoclave was cooled to room temperature, methanol and water were used to filter the black particles multiple times. The mixture was then dried for 24 hours at 80 °C.

3.3 Synthesis of MXene

MXene was synthesized by the process of etching. This process used ammonium fluoride (NH_4F) as an etching agent to produce MXene. At room temperature (298 K), 0.5 g of MAX phase powder (Ti_3AlC_2) that had been sieved with 200 screen was slowly immersed in 100 ml of 1 M NH_4F. The mixture was then agitated for a whole day. After centrifuging the sedimented solids for 15 minutes at 6000 rpm, the pollutants were entirely removed using deionized water, and the dispersion's pH was stabilized at around 7. In order to create the synthesized $Ti_3C_2T_x$ MXene, the filtrate was dried for 24 hours at 60 °C in a vacuum oven and then stored for later use.

3.4 Preparation of Cr(VI) Stock Solution

Chromium stock solution was prepared using potassium dichromate ($K_2Cr_2O_7$). In a 1000 mL volumetric flask, 2.83 g of $K_2Cr_2O_7$ (99% purity) was dissolved into 1000 mL of deionized water to freshly prepare 1000 mg/L Cr(VI) stock solution. After giving the mixture a good shake, it was put to use in other experiments.

3.4.1 Preparation of Calibration Curve

For calibration curve, prepare Cr solutions of different known concentrations to get the concentration of an unknown solution. The curve was prepared by using UV Vis Spectrophotometer.

3.4.1.1 Reagents used

- DPC(Diphenyl carbazide)

- Acetone

- Orthophosphoric acid

3.4.1.2 Preparation of chromophoric reagent

Dissolve 250 mg of DPC in 50 ml acetone in an airtight brown bottle.

3.4.1.3 Solution Preparation for analysis of hexavalent chromium using UV Vis Spectrophotometer

Add 2 to 3 drops of orthophosphoric acid to the prepared solution. Leave the solution for 1 to 2 minutes and then add 2 ml of the above prepared chromophoric reagent into it. The color of the solution will turn pink. Repeat the same procedure for Cr solution of 0.5, 1, 1.5, 2, 2.5, 3 mg/L (Table 3.1). Then, check the absorbance of each solution through spectrophotometer and get the required calibration curve.

Table 3.1: Data for calibration curve

Concentration (mg/L)	Absorbance
0.5	0.4225
1	0.8714
1.5	1.2663
2	1.6229
2.5	1.9797
3	2.3416
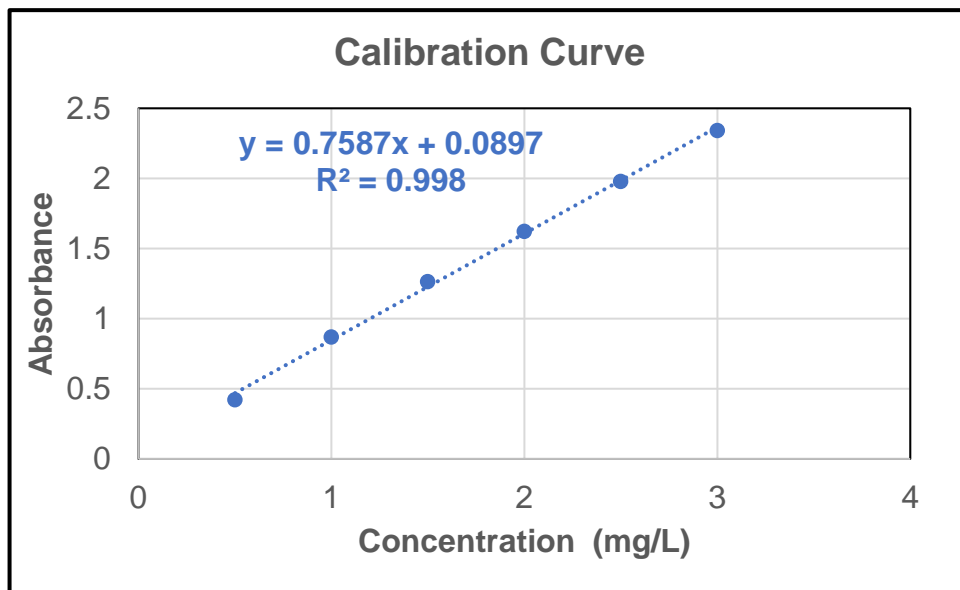
Figure 3.1: Calibration Curve

3.5 Batch Adsorption Measurements

In the adsorption experiments for the removal of chromium, batch technique was applied. In a typical procedure, 5 mg of MoS_2 and 10 mg of MXene was immersed in 10 mL of chromium solution with concentration varying from 20 mg/L to 120 mg/L, respectively, and shaken at 120 rpm at 298K. After adsorption, solid residue was separated using 0.2 μm syringe filters. The supernatant was further used for measuring adsorbent's removal efficiency. Cr(VI) concentration was measured using the standard curve shown in (Figure 3.1) using UV vis spectrophotometer by diphenyl carbazide method at a wavelength of 540 nm (Jin et al., 2020). After adsorption, adsorbents were washed with deionized water and desorption reagent (0.1 M NaOH) for recycling experiments. To check the effect of pH, pH tests were conducted by adjusting pH from 2 to 8 using 0.1 M HCl and 0.1 M NaOH solutions. Kinetics studies were

conducted at a fixed concentration of 30 mg/L at 298K for designated time. Also, the ionic strength of different cations and anions was applied to study the effect of competitive ions on Cr(VI) removal. All the kinetics and isotherm studies were conducted at 3 different temperatures (25 °C, 35 °C, 45°C) for thermodynamic studies. At last, the removal efficiency and adsorption capacities were measured for chromium by MoS$_2$ and MXene, respectively, using the following equations.

3.5.1 Adsorption Capacity

$$Q_e = (C_o - C_e) \times V/m \qquad (3.1)$$

3.5.2 Removal Percentage

$$R = (C_o - C_e)/C_o \times 100\% \qquad (3.2)$$

where C$_o$ is the pollutant's (CrVI) initial concentration, C$_e$ is the final concentration, V is the working volume and m is the mass of adsorbent used in the experiment.

3.6 Material Characterization of MoS$_2$ and MXene

The morphology of the synthesized adsorbents was analyzed by Scanning Electron Microscopy (SEM) (JSM6940LA Analytical Low Vacuum SEM). The functional groups on the adsorbents were characterized through Fourier-transform infrared (FTIR) spectroscopy (PerkinEimer Spectrum 100 FTIR Spectrophotometer) in the range of 400 to 4000 cm^{-1}. The crystalline nature of the adsorbents was studied through acquiring their powder X-ray diffractograms using an X-ray diffraction (XRD) spectrometer (BRUKER 2D Phaser) in the 2θ range from 0º to 80º. The specific surface area, pore volume, and pore size distribution of the samples (degassed at 180°C for 24 hours) were determined by the Brunauer–Emmett–Teller (BET) method using a surface area analyzer (Gemini VII 2390t, Micromeritics). The zeta potential measurements were conducted using a zeta potential analyzer (Wallis Zeta Potential Analyzer, Cordouan Technologies.

CHAPTER 4: RESULTS AND DISCUSSION

4.1 Material Characteristics of the Synthesized Adsorbents

4.1.1 XRD Analysis

XRD analysis of MXene and MoS_2 was performed to assess the crystalline structures and interlayer spacing of the particles. An intense peak of Ti_3AlC_2 appears at $2\theta = 39°$ corresponding to (104) in Ti_3AlC_2. Other peaks of Ti_3AlC_2 are shown at $9.33°$, $19.25°$, $33.82°$, $41.61°$ corresponding to (002), (004), (003) and (105) respectively. As the MXene was etched by NH_4F, the peak at (104) disappeared and a new peak is seen at $27.3°$ corresponding to (008) diffraction. An undefined peak of TiC impurity was seen at $38°$ as shown in Figure 4.1A. XRD results of MXene are consistent with standard pattern (JCPDS no: 52-0875). Moreover, after etching, the peak of MXene is moved towards the smaller angle and gets broaden which confirms the enlarged interlayer spacing in MXene (Kong et al., 2021). From the XRD results, it can be concluded that etching of Ti_3AlC_2 with NH_4F resulted in the weakening of Ti-Al metal bond and removed the Al element from MAX phase (Jamaluddin et al., 2022).
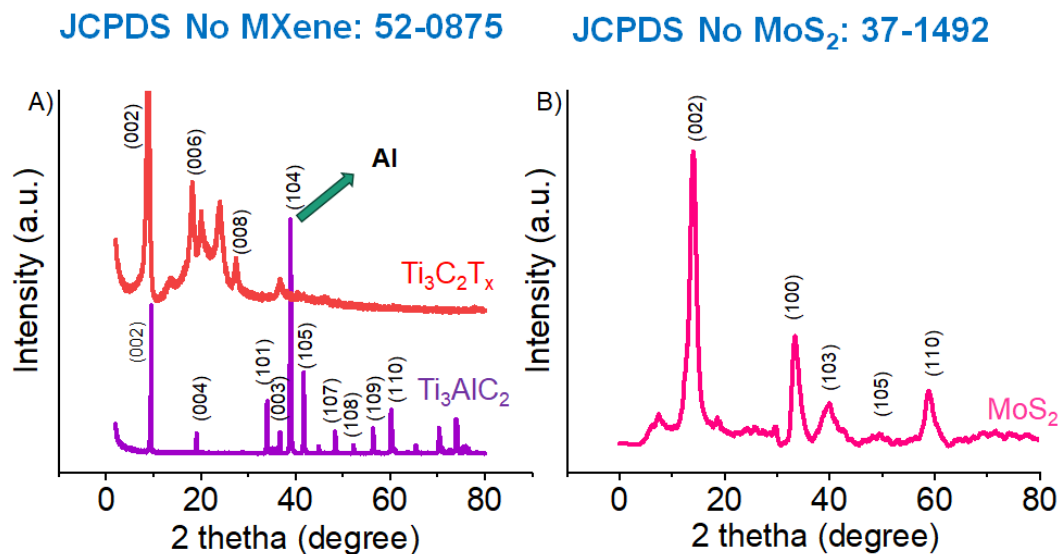
Figure 4.1: XRD analysis of (A) MXene and (B) MoS_2.

XRD peaks of MoS_2 at diffraction angles of $14.2°$, $33.4°$, $39.6°$, $49.36°$, and $58.86°$ respectively correspond to (002), (100), (103), (105), and (110) signature peaks of MoS_2 Figure 4.2B. Pattern of MoS_2 are in good agreement to the standard XRD pattern (JCPDS no: 37-1492). Peak of (002) shows the formation of multiple layers along (002) direction. The formation of

peak at 14.2° is formed due to the scattering of Mo-Mo atomic layers in the MoS_2 interlayer whereas other peaks at 33.4°, 39.6°, 49.36°, and 58.86° are formed due to interlayer interactions (Xiang et al., 2021). The XRD results confirm the successful synthesis of crystalline MXene and MoS_2 as reported in the literature.

4.1.2 SEM Analysis
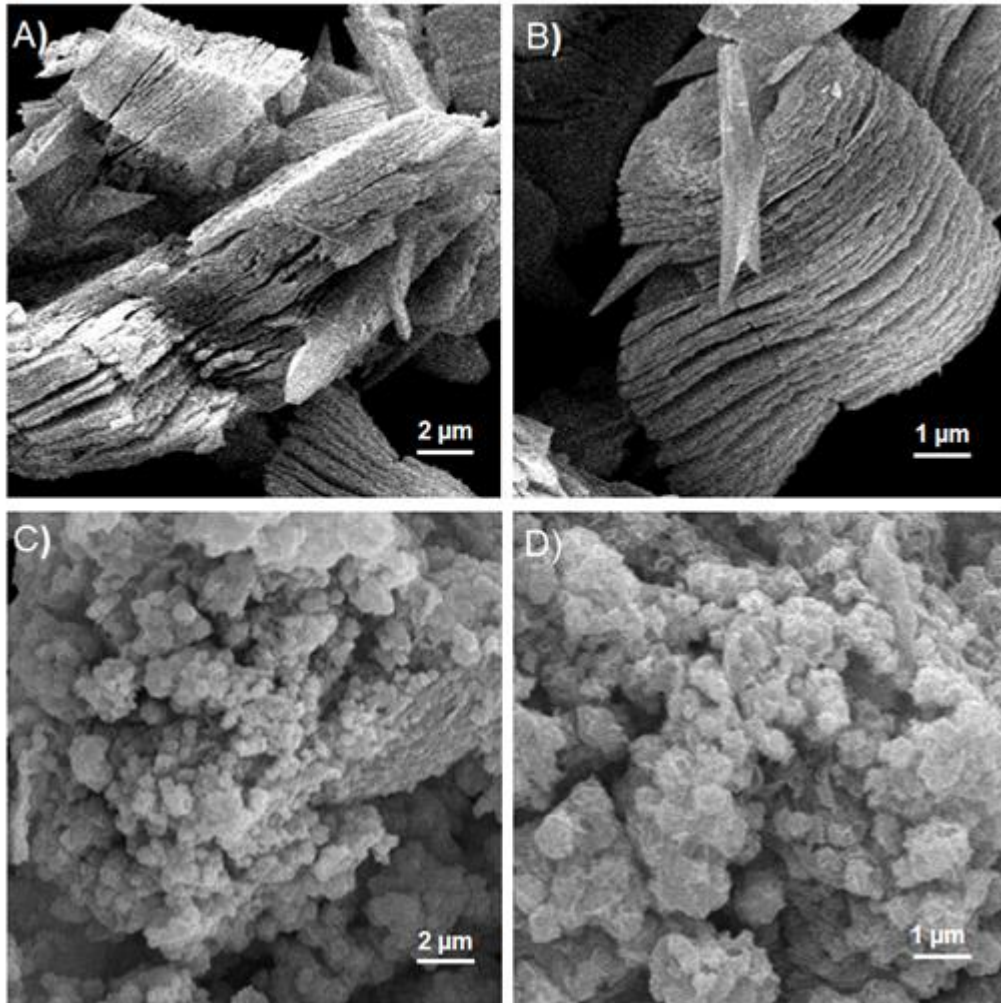
Figure 4.2: SEM images of (A-B) MXene and (C-D) MoS_2 at different magnifications.

Morphologies of MoS_2 and MXene were analyzed by Scanning Electron Microscope. SEM analysis of the MXene showed thin layered surface arrangement Figure 4.2A representing lamella like structure Figure 4.2B. The accordion-like structures of the synthesized MXene represent the splitting of layers as compared to Ti_3AlC_2 which exhibits a brick like structure with compacted layers connected with strong metallic bonds of Titanium and Aluminium (Kong et al., 2021). Figure 4.2C and 4.2D show the flower-like structure of MoS_2 at a scale of 2 μm and 1 μm, respectively. The interconnected spherical MoS_2 particles indicate a porous

material structure. This porosity of clustered nanoparticles is often associated with better adsorption performance of Cr(VI) (Sun et al., 2018). The results reported in this research for both the nano materials are mostly similar to those reported in the literature (Kong et al., 2021; Sun et al., 2018).

4.1.3 EDS Analysis

Element	Weight%	Atomic %
C K	20.8	38.6
N K	2.1	4.0
O K	11.6	16.9
F K	2.9	5.4
Ti K	62.6	35.1
Total	100	100

Element	Weight%	Atomic %
C K	2.8	30.9
O K	2.6	10.7
S K	36.2	37.2
Mo L	58.4	21.2
Total	100	100
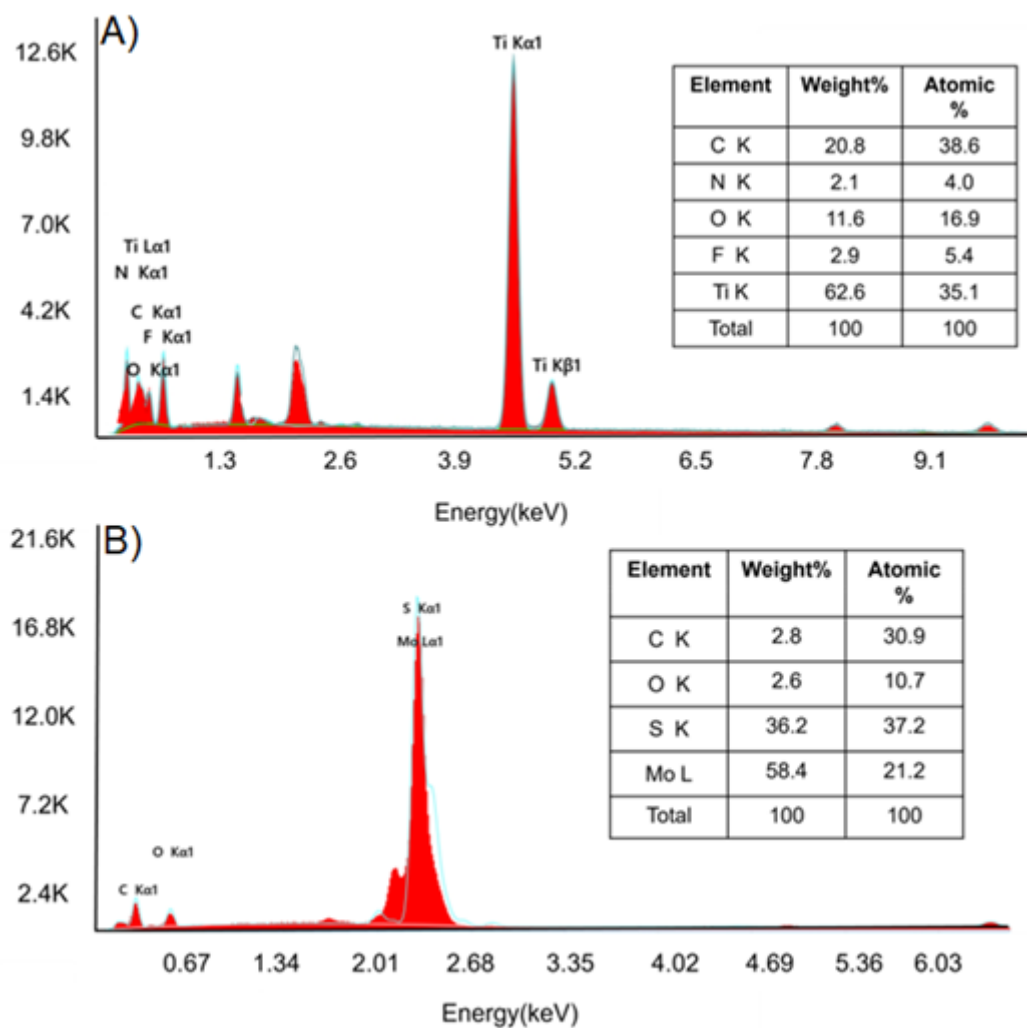
Figure 4.3: EDS analysis of (A) MXene and (B) MoS$_2$.

EDS analysis of MXene shows that Al is decreased Significantly after etching with NH$_4$F and the layers are spaced apart. The removal of Al verifies the formation of MXene and presence of surface terminations of functional groups such as O, and fluorine groups (Figure 4.3A). In the case of MoS$_2$ (Figure 4.3B), it can be seen that the sample majorly comprises of Mo and S. The elemental composition determined from EDS for MoS$_2$ constitutes S (58.4%), O (2.6%),C (2.8%), and S (36.2%), while for MXene, it includes Ti (62.6%), C (20.8%), O (11.6%), and F (2.9%).

4.1.4 FTIR and BET Analysis

FTIR is a characterization technique to characterize surface structure and associated functional groups of any sample. Figure 4.4A shows the FTIR spectrum of MXene before adsorption in which a clear peak of OH$^-$ group appears at 3435 cm^{-1} confirming the formation of hydroxyl functional groups on the surface of synthesized MXene. Other typical peaks of MXenes appeared at 1637 cm^{-1}, 1289 cm^{-1}, 868.76 cm^{-1}, and 544 cm^{-1} representing H-OH, C-H, C=O, and Ti-O respectively. After the adsorption of Cr(VI), the intensities of functional groups on the surface of MXenes were weakened. The intensity of -OH group decreased, and the peak shifted from 3435 cm^{-1} to 3444 cm^{-1} which shows the interaction of OH group and Cr during adsorption (He et al., 2020). The broadband at 1628 cm^{-1} is attributed to H-OH stretching vibrations of MXenes (Karthikeyan et al., 2021). Similarly, the shifts in other peaks with reduced intensity after the adsorption confirms further that Cr(VI) is successfully adsorbed on the surface of MXenes. Unlike MXenes, the spectrum of MoS$_2$ before adsorption (Figure 4.4B)
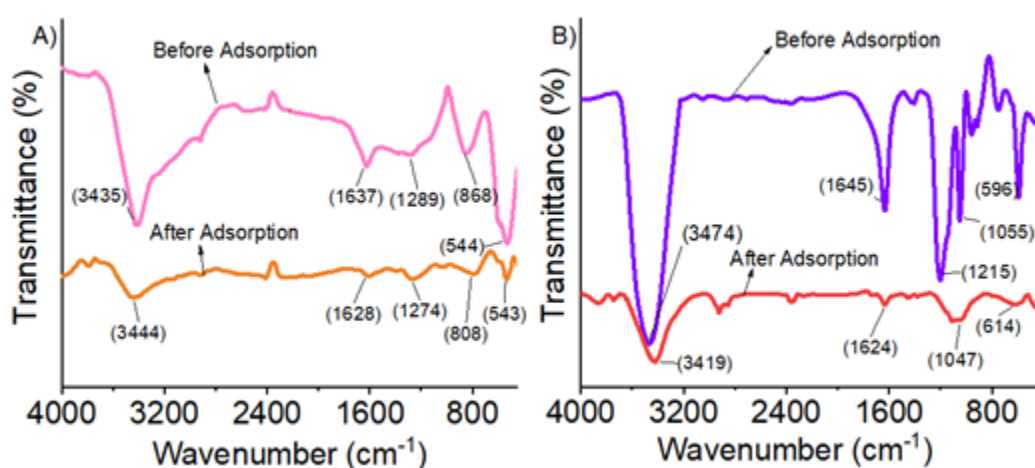
Figure 4.4: FTIR analysis of (A) MXene and (B) MoS$_2$ before and after Cr(VI) adsorption.

showed a peak at 596 which corresponds with Mo-S stretching vibrations (Chen et al., 2022). Peaks at 1055 cm^{-1} and 1215 cm^{-1} were associated with C-N-H stretching vibrations (Xiang et al., 2021) which merged and shifted to 1047 cm^{-1} after adsorption. Peak at 1645 cm^{-1} shows the bending vibrations of hydroxyl group (-OH) (Xiang et al., 2021). Peak at 3474 cm^{-1} before adsorption is attributed to stretching vibrations of hydroxyl group which shifted to 3419 cm^{-1} with reduced intensity after adsorption (Wang et al., 2018). The shifts occurring in the FTIR spectrum of MoS$_2$ after adsorption indicate that chemical interactions occur between the MoS$_2$

adsorbent and Cr(VI) (Cai et al., 2020). The BET analysis showed that the surface area of MXene and MoS_2 was 5.35 and 4.68 m^2/g, respectively.

4.2 Effect of Operational Parameters on Adsorption of Cr(VI) onto MXene and MoS₂

Many batch experiments were performed to check the influence of different parameters on the adsorption of chromium onto MXene nanosheets and pure MoS_2.

4.2.1 Effect of Solution pH on Adsorption

The pH of solution is a very essential parameter in determining the speciation of chromium in water as it controls the ionic forms and valence states of heavy metals. The effect of pH ranging from pH (2 to 8) on both MXene and MoS_2 is shown in Figure 4.5A and 4.5B respectively. It can be seen that the maximum removal of MXene and MoS_2 is shown at pH 2 whereas the increase in pH of solution decreases the adsorption capacity which confirms that the pH greatly influences the removal capacity of adsorbent. Similarly, for MoS_2, the removal of Cr(VI) shows strong dependency on pH as maximum removal of Cr(VI) is found at pH 2 after 90 minutes. When the pH of solution was increased to pH 8, the adsorption capacity is reduced to 26.98 mg/g. Chromium dissociates into different oxyanions in water.

$$H_2CrO_4 \quad \leftrightarrows \quad HCrO_4^- + H^+ \qquad (4.1)$$

$$Cr_2O_7^{2-} + H_2O \leftrightarrows 2HCrO_4^- \qquad (4.2)$$
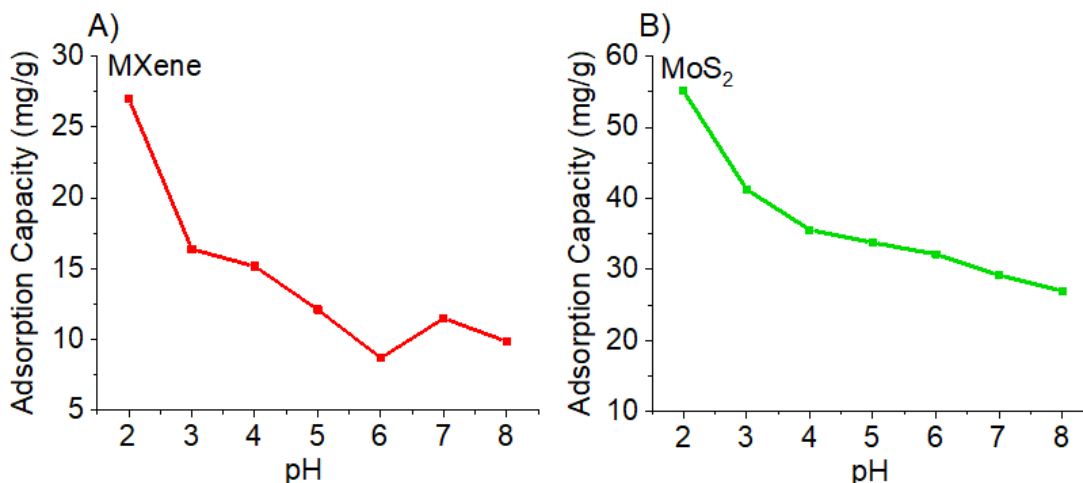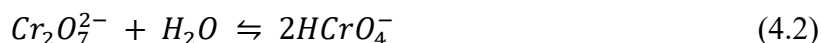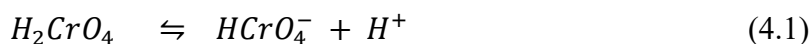
Figure 4.5: Effect of pH on adsorption capacity (A) MXene (C_o = 30 mg/L, T = 298 K, Time = 9 h, Dosage = 1 g/L) and (B) MoS_2 (C_o = 30 mg/L, T = 298 K , Time = 1.5 h, Dosage = 0.5 g/L).

The existence of different ions for Cr(VI) is regulated by pH. Within the pH range of 2-6, the dominant species of chromium are $Cr_2O_7^{2-}$ and $HCrO_4^-$ and at pH > 6, CrO_4^{2-} species become dominant in water (Wang et al., 2018). H_2CrO_4 dominates at pH < 1 (Feng et al., 2021). The zeta potential values are also maximum at pH 2 for both MXene and MoS_2 which indicates the higher percentage of $HCrO_4^-$ over $Cr_2O_7^{2-}$ at lower pH value (Zeng et al., 2021). The change in zeta potential values of MXene and MoS_2 at different pH values is shown in Figure 4.6. MXenes show good chromium removal in acidic pH due to the protonation of the surface of MXene nanosheets (Karthikeyan et al., 2021). In the case of MoS_2, the addition of PVP during synthesis process induces positive charge on its surface (Baig et al., 2020). This makes it highly protonated due to the strong electrostatic force of attraction between adsorbate and adsorbent in aqueous media. Acidic pH is more favorable in the removal of chromium (Wang et al., 2020). Based on these results, pH 2 was taken as the optimum pH for both adsorbents which was further applied in the following studies.
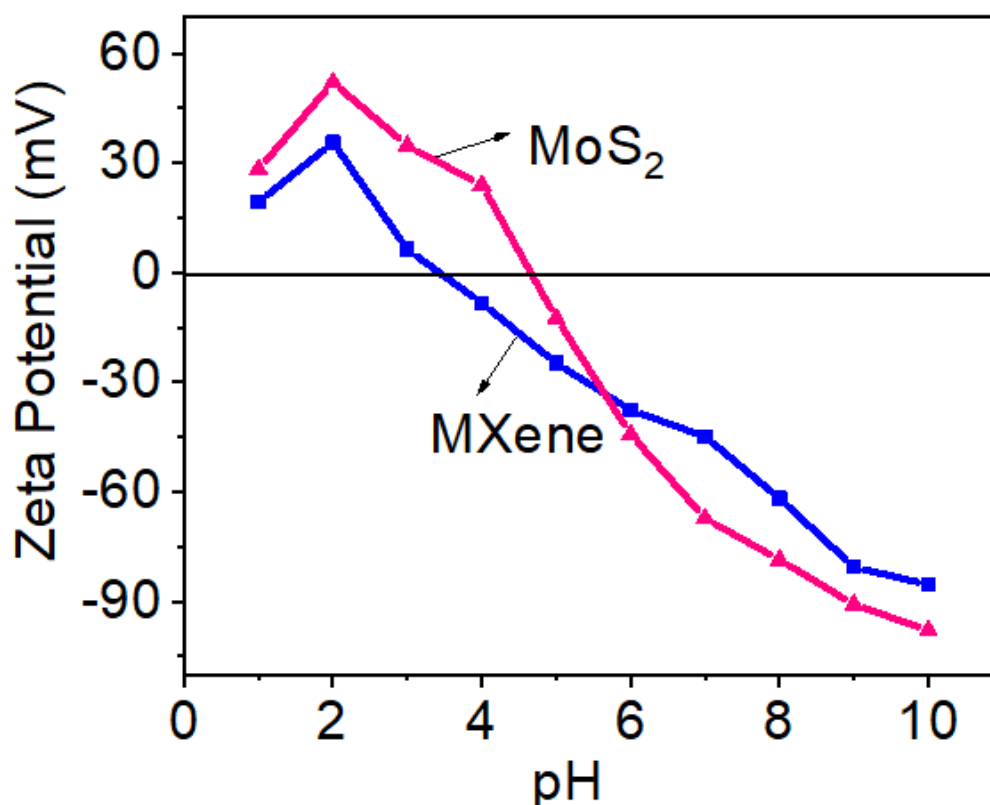
Figure 4.6: Zeta Potential measurements of MXene and MoS_2.

4.2.2 Effect of Adsorbent's Dosage on Adsorption

At MXene (Figure 4.7A) and MoS$_2$ (Figure 4.7B), the impact of adsorbent dosage was examined using dosages of materials ranging from 0.1 to 2 g/L and 0.1 to 0.7 g/L, respectively, while maintaining concentration of Cr(VI) at 30 mg/L, solution temperatures of 298 K for both MXene and MoS$_2$ and pH = 2. In the case of MXene (Figure 4.7A), the adsorption capacity decreased sharply from 53.86 mg/g to 19.86 mg/g with an increase of dosage from 0.1 g/L to 1.2 g/L. The adsorption rate was maximum with further increase in dosage up to 2 g/L indicating almost complete removal of Cr(VI). Similarly, for MoS$_2$, the adsorption capacity of chromium was decreased from 71.14 mg/g to 42.75 mg/g with adsorbent dosage varying from 0.05 g/L to 0.6 g/L which was further decreased to 40.77 mg/g at 0.7 g/L MoS$_2$. The optimum dosage value chosen for MXene and MoS$_2$ was 1 g/L and 0.5 g/L, respectively, for further experimentation.
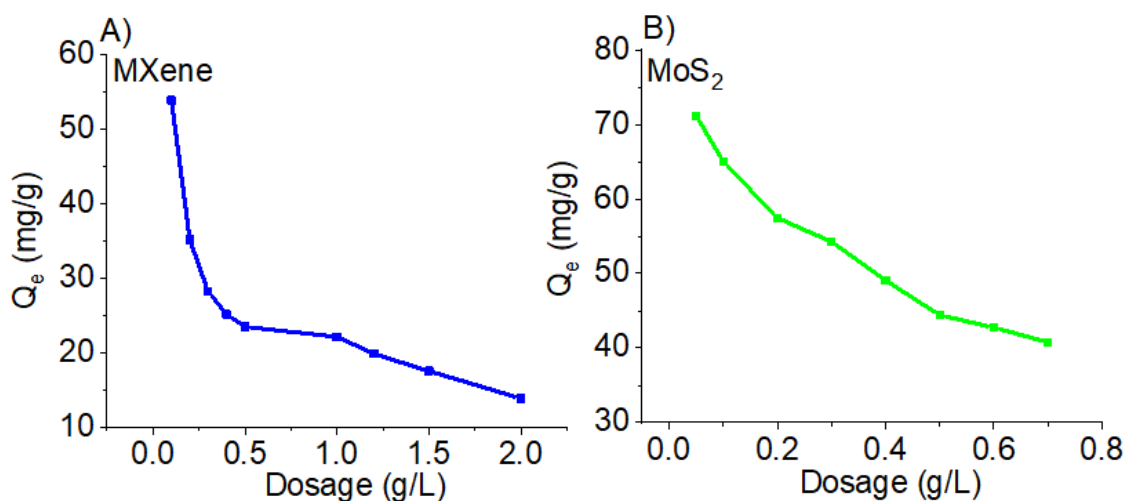
Figure 4.7: Dosage effect on removal percentage and adsorption capacity.(A), (B) MXene (C$_o$ = 30 mg/L, T = 298 K, Time = 9 h, pH = 2) and (C), (D) MoS$_2$ (C$_o$ = 30 mg/L, T = 298 K , Time = 1.5 h, pH = 2)

4.2.3 Effect of Contact Time on Adsorption

This study aims to analyze the effect of time on the adsorption of MXene and MoS$_2$ and the results are shown in Figure 4.8A and 4.8B respectively. Adsorption of Cr(VI) was performed at MXene dosage of 1 g/L and MoS$_2$ dosage of 0.5 g/L, an initial chromium concentration of 30 mg/L, temperature of 298 K, 308 K and 318 K, and pH value of 2. Q$_e$ achieved after 9 hours was 24.34 mg/g for MXene and Q$_e$ achieved for MoS$_2$ was 47.10 mg/g after 90 minutes. Chromium removal was faster by MoS$_2$ as compared to MXene. The enhanced chromium

adsorption of MoS$_2$ is due to the unique structural arrangement of MoS$_2$ with enlarged interlayer spacing. The defects in the structure acted as permeable channels in the diffusion of ions in the bulk of MoS$_2$. Moreover, the average pore diameter of MoS$_2$ is larger than MXene which provides more active sites for the adsorption of Cr(VI). Upon saturation of MXene and MoS$_2$, the uptake of Cr(VI) decreases and finally equilibrium is achieved.

4.3 Kinetics of Cr(VI) Adsorption onto MXene and MoS$_2$
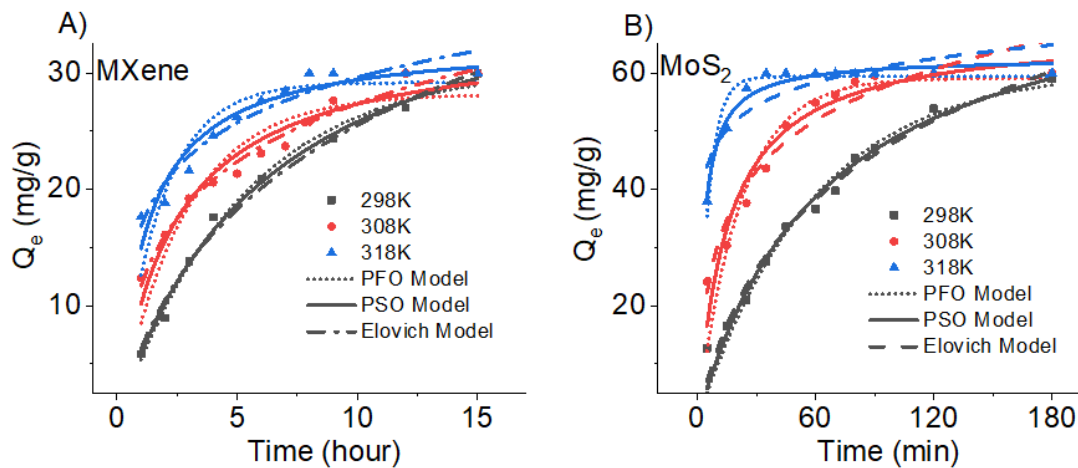
Figure 4.8: Effect of time on Cr(VI) adsorption and nonlinear kinetics of different models (PFO, PSO, Elovich) for Cr(VI) adsorption (A) MXene and (B) MoS$_2$.

Reaction time determines the efficiency of the absorbent in its practical application. Therefore, two dimensional nanomaterials MXene and MoS$_2$ were selected to check their performance for Cr(VI) removal. Compared to MoS$_2$, longer time was taken by MXene to achieve adsorption equilibrium with lower adsorption capacity. In order to research both material's adsorption rate and their role in potential rate limiting steps, linear and nonlinear kinetics of different models were applied on both materials. The following equations were used to compute the kinetics curves for Cr(VI) adsorption at three different temperature values on MXene and MoS$_2$ for the pseudo first order, pseudo second order, Elovich model and Intraparticle Diffusion Model.

4.3.1 Pseudo-First Order

$$Q_t = Q_e (1 - exp(-k_1 t)) \quad \ldots\ldots\ldots\ldots\text{Linear} \tag{4.4}$$

$$log(Q_e - Q_t) = (log(Q_e) - k_1 t / 2.303) \quad \ldots\ldots\ldots\text{Non–Linear} \tag{4.5}$$

where k_1 denotes pseudo first order rate constant, Q_t represents the adsorption capacity (mg/g) at equilibrium and Q_t represents the adsorption capacity at time t, (min) for MoS$_2$ and (hour) for MXene.

4.3.2 Pseudo-Second Order

$$Q_t = Q_e^2 k_1 t \,/\, Q_e k_2 t + 1 \ldots\ldots\ldots\ldots\ldots\text{.Linear} \tag{4.6}$$

$$t/Q_t = (1 \,/\, k_2 Q_e^2 + t/Q_e) \ldots\ldots\ldots\ldots\text{.Non–linear} \tag{4.7}$$

Where k_2 denotes pseudo second order rate constant, Q_t represents the adsorption capacity (mg/g) at equilibrium and Q_t represents the adsorption capacity at time t, (min) for MoS$_2$ and (hour) for MXene.

4.3.3 Elovich Model

$$Q_t = 1 \,/\, \beta ln \,(1 + \beta\,\alpha) \ldots\ldots\ldots\ldots\ldots\ldots\text{.Linear} \tag{4.8}$$

$$Q_t = \beta ln(t) + \beta ln(\alpha) \ldots\ldots\ldots\ldots\text{.Non-Linear} \tag{4.9}$$

where Q_t is the adsorption capacity of Cr(VI) at time t, (min) for MoS$_2$ and (hour) for MXene. α is for the primary rate of adsorption. β represents desorption parameter and is used to characterize the activation energy and degree of chemisorption.

4.3.4 Intraparticle Diffusion

$$Q_t = K_{ip}\, t^{1/2} + C \tag{4.10}$$

The nonlinear kinetics curves are shown in figure 4.8A and Figure 4.8B whereas the fitting curves for linear kinetics are shown in Figure 4.9 and Figure 4.10 for MXene and MoS$_2$ respectively. All the chi square values and kinetic parameters of MXene and MoS$_2$ adsorbents are shown in Table 4.1 and Table 4.2.
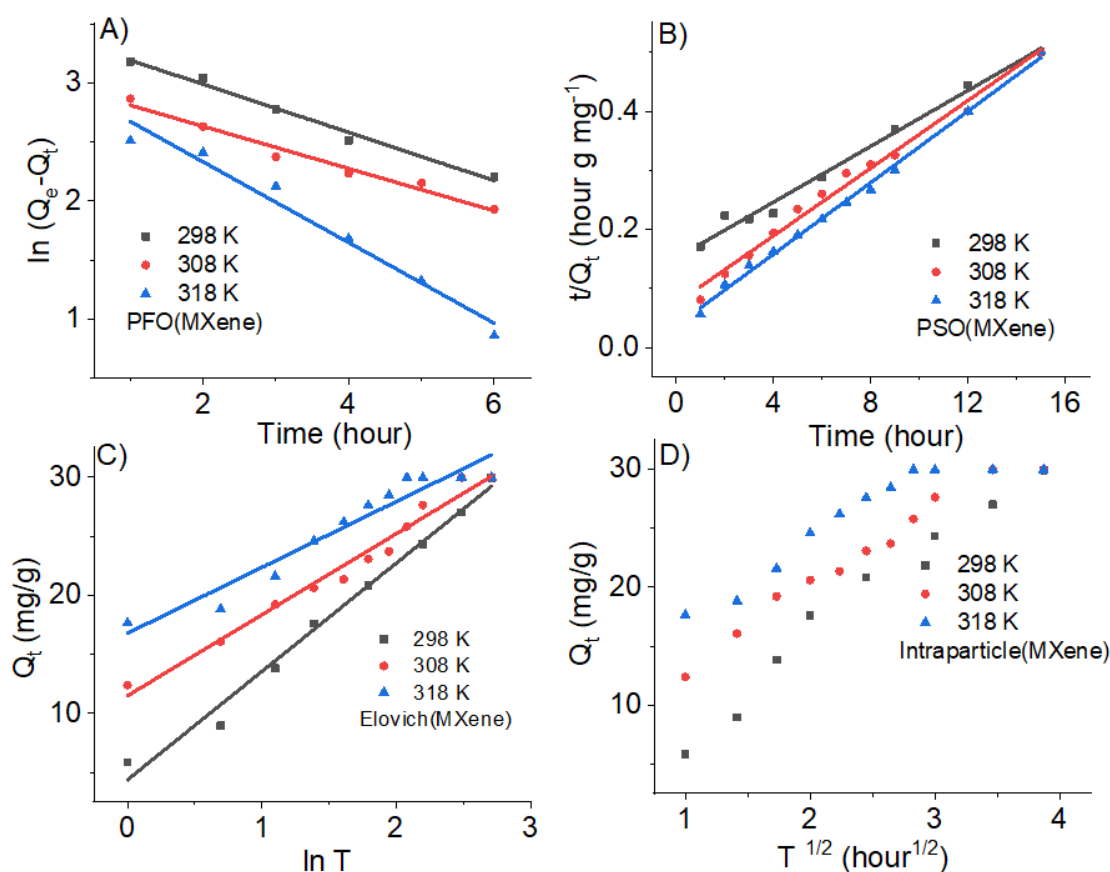
Figure 4.9: Linear kinetics of different models (A) PFO, (B) PSO, (C) Elovich, (D) Intraparticle Diffusion for Cr(VI) adsorption by MXene at T = 298 K, 308 K, 318 K.

From the tables, it can be clearly observed that the linearized and non-linearized pseudo second order shows higher values of correlation coefficients of R^2 for MXene and MoS_2, respectively than pseudo first order and Elovich model. The pseudo-second order Q_e values that are computed also fit well with the experimentally determined Q_e values. Additionally, Q_e calculated by the non-linearized equation is well suited to $Q_{e\ exp}$ than linearized equation which suggests that experimental data is more coherent to non- linearized pseudo second order kinetic model then linearized one. Additionally, the pseudo second order model's computed values of X^2 are lower than those of the pseudo first order model, confirming the suitability of the pseudo second order model for the adsorption kinetics process and suggesting that chemisorption for both MXene and MoS_2 is a part of the adsorption process.
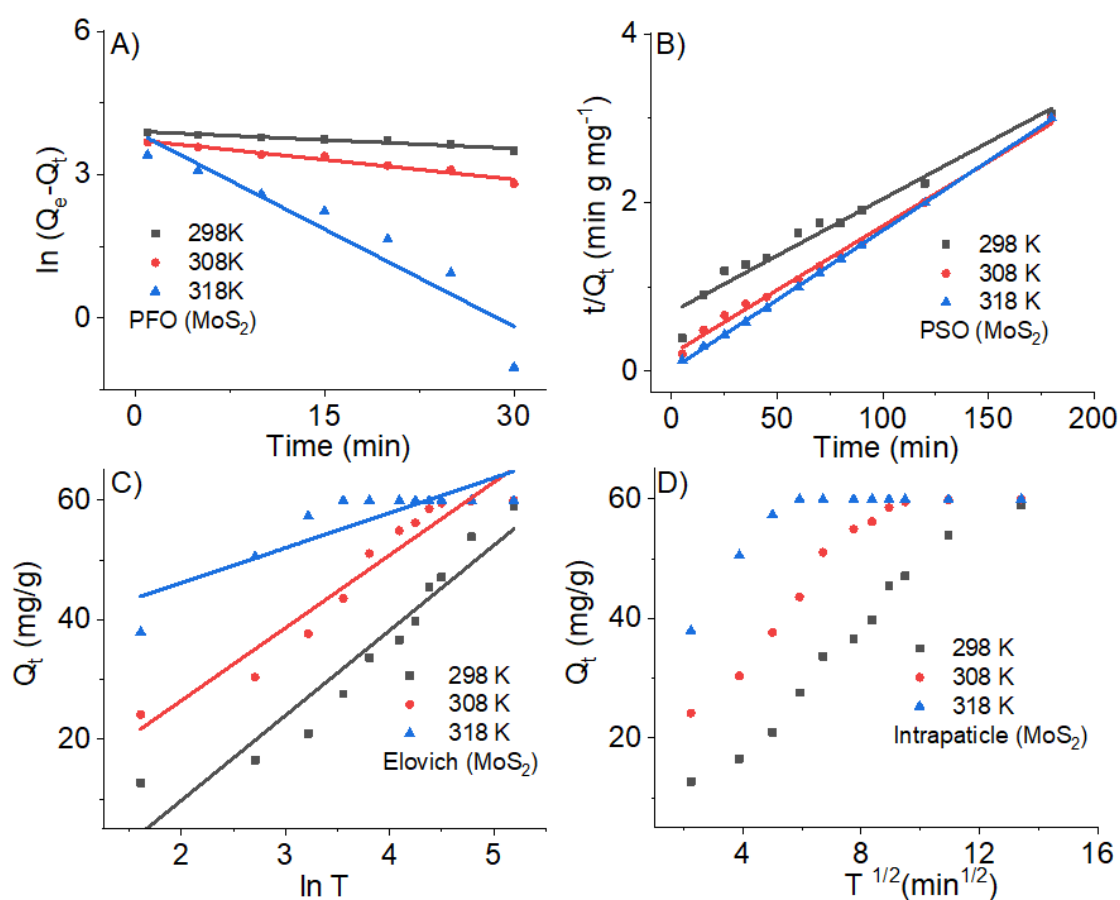
Figure 4.10: Linear kinetics of different models (A) PFO, (B) PSO, (C) Elovich, (D) Intraparticle Diffusion for Cr(VI) adsorption by MoS$_2$ at T = 298 K, 308 K, 318 K.

Table 4.1: PFO and PSO kinetics parameters for Cr(VI) adsorption by MXene and MoS$_2$

Kinetic Model	Adsorbent					
	MXene Temperature (K)			MoS$_2$ Temperature (K)		
	298	308	318	298	308	318
Pseudo-first order						
$(Q_e)_{exp}$	29.93542	29.96441	29.98155	59.00092	59.98946	59.99501
Linear						
(Q_e)cal	29.8865	20.1136	20.47542	49.89994	41.69299	49.6793
K_1	0.46966	0.42731	0.79213	0.02757	0.06355	0.31327
R^2	0.98103	0.97456	0.95379	0.93195	0.95533	0.87667
Non-Linear						
Best fit values						
(Q_e)cal	30.64025	28.92704	29.12255	60.73888	59.11846	59.40416
K_1	0.19352	0.3695	0.58034	0.01709	0.04633	0.18091
R^2	0.98987	0.89601	0.7718	0.9598	0.88484	0.91768

Kinetic Model	Adsorbent					
	MXene Temperature (K)			MoS$_2$ Temperature (K)		
	298	308	318	298	308	318
X^2	0.7477	4.5493	4.34572	9.24451	19.0286	3.90276
Std.error						
(Q_e)cal	0.98041	1.34465	1.29228	3.50836	2.1617	0.65795
K_1	0.01459	0.05434	0.10141	0.00214	0.00665	0.01562
Goodness of fit						
Degrees of freedom	6	6	6	9	9	9
Number of points Analyzed	8	8	8	11	11	11
Pseudo-second order						
Linear						
(Q_e)cal	42.28157	34.8594	32.8795	74.54213	65.85134	60.78934
K_2	0.00369	0.01196	0.0246	0.000256	0.00112	0.01055
R^2	0.98653	0.9927	0.9966	0.95058	0.99419	0.99964
Non-Linear						
Best fit values						
(Q_e)cal	41.62159	34.20287	32.5032	80.18667	67.32323	62.66437
K_2	0.00392	0.01285	0.02636	0.000193	0.000965	0.00512
R^2	0.9917	0.96107	0.90402	0.96862	0.92688	0.95976
X^2	0.6126	1.64606	2.5373	7.21515	12.08289	1.90758
Std. error						
(Q_e)cal	1.81717	1.43039	1.30848	5.77509	2.8111	0.6285
K_2	0.00018	0.00232	0.00587	0.00004	0.00020	0.0005
Goodness of fit						
Degrees of freedom	6	6	6	9	9	9
Number of points Analyzed	8	8	8	11	11	11

Units: K_1: 1/h; K_2: g/mg/h (Q_e)exp, (Q_e)cal: mg/g, (MXene)

Units: K_1: 1/m; K_2: g/mg/m (MoS$_2$) ,(Q_e)exp, (Q_e)cal: mg/g,(MoS$_2$)

Table 4.2: Elovich model kinetic parameters for Cr(VI) adsorption by MXene and MoS_2

Kinetic Model	Adsorbent					
	MXene Temperature (K)			MoS_2 Temperature (K)		
	298	308	318	298	308	318
Elovich model Linear						
A	0.10899	0.14578	0.17933	0.07036	0.08218	0.171
B	40.11051	78.80637	93.56995	265.2249	25.96045	201.58136
R^2	0.98519	0.97345	0.92278	0.90519	0.92549	0.72342
Non-Linear Best fit values						
A	8.15968	29.13768	112.37741	1.64315	12.04337	2127.60783
B	0.0784	0.13308	0.18316	0.04368	0.07814	0.17105
R^2	0.98764	0.98726	0.93686	0.97338	0.92697	0.72336
X^2	0.91258	0.5385	1.66924	6.12093	12.06753	13.11528
Std.error						
A	0.85372	3.73571	44.27588	0.22049	3.98903	3601.12547
B	0.00699	0.0073	0.01927	0.00472	0.0084	0.03305

Units: MXene: α = g mg^{-1} h^{-1} , β = g/mg

Units: MoS_2: α :g mg^{-1} m^{-1} , β = g/mg

Additionally, pseudo first order, pseudo second order and Elovich model do not explain the diffusion mechanism of Cr(VI) removal. As a result, Weber and Morris' inter particle diffusion model was applied at 298 K, 308 K, and 318 K to study the diffusion process and rate-limiting steps of the adsorption process on MXene and MoS_2 as shown in Figure 4.9D and Figure 4.10D, respectively. Q_t is the Cr(VI) adsorbed quantity at time t (mg/g), k_{ip} stands for the rate constant of the model, (g/mg/time), t is for the contact time which is (min) for MoS_2 and (hour) for MXene and C denotes the intercept written as (mg/g). Different intraparticle diffusion rate constants such as k_{ip} and C were calculated at three temperature values using slope and intercept values of the graphs and the results are shown in Table 4.3. Based on the data, it can be inferred that the boundary layer's influence on the surfaces of MXene and MoS_2 is what caused the first adsorption. Adsorption is redirected towards porous diffusion on the interior structures of MXene and MoS_2 as the active sites on their surface decrease. At the end stages of adsorption curve, adsorption reaches equilibrium as shown in Figure 4.9D and Figure 4.10D for MXene and MoS_2, respectively. As a result, the adsorption process involves two different types of diffusion mechanisms i.e. adsorption on surface and internal diffusion.

Table 4.3: Intraparticle diffusion model kinetic parameters for Cr(VI) adsorption by MXene and MoS$_2$.

Kinetic Model	Adsorbent					
	MXene Temperature (K)			MoS$_2$ Temperature (K)		
	298	308	318	298	308	318
Intraparticle diffusion model						
Linear						
A	0.10899	0.14578	0.17933	0.07036	0.08218	0.171
K$_{diff}$	8.36098	6.3407	4.97166	4.64345	3.639	1.50704
C	1.23946	7.35222	13.86036	0.85133	21.36579	45.53085
R^2	0.96873	0.96689	0.84499	0.97276	0.81524	0.44264
Non-Linear						
Best fit values						
K$_{diff}$	7.9097	6.31923	4.80513	4.64345	3.639	1.50704
C	1E-14	7.4111	13.65879	0.85133	21.36579	45.53085
R^2	0.96489	0.96559	0.88046	0.97276	0.81524	0.44264
X^2	2.5918	1.45499	3.16013	6.26365	30.52888	26.4237
Std. error						
K$_{diff}$	0.22325	0.44974	0.6628	0.24538	0.54172	0.50398
C	0	1.14662	1.68982	1.99208	4.39793	4.09157

4.4 Effect of Cr (VI) Concentration on Adsorption

A comparative study for optimizing the optimal conditions for the removal of Cr(VI) was conducted for both MXene and MoS$_2$. To check the effect of concentration of pollutant on the adsorption capacities of both adsorbents, seven Cr(VI) concentrations ranging from 20 mg/L to 120 mg/L were used and the results are shown in Figure 4.11A of MXene and Figure 4.11B of MoS$_2$. As seen in the figures, adsorption capacity of MXene and MoS$_2$ enhanced with increase of Cr(VI) concentration and rapid increase in the adsorption capacities at early stages may be attributed to excess of unoccupied adsorption sites on the surface of adsorbents at lower concentrations. But with increasing concentration of Cr(VI), the number of adsorption sites on the surface of adsorbent declined and behaved as limiting step for the Cr(VI) adsorption (Shahzad et al., 2017; Harijan & Chandra., 2016).

4.5 Adsorption Isotherm Study

To study the interaction of adsorbate on the surface of adsorbent, isotherm models are studied. In this study, adsorption isotherm was fitted using Langmuir, Freundlich and Tempkin

isotherms models at three different temperatures 298 K, 308 K and 318 K as shown in Figure 4.11A and 4.11B. Experimental data was simulated using Langmuir, Freundlich and Tempkin isotherms to better understand the adsorption process and determine the highest adsorption capacities. The linearized and non-linearized equations of all the three models applied are as follows.

Langmuir Isotherm Model describes that maximum adsorption is due to monosaturated layer of adsorbate on the surface of adsorbent. The energy of adsorption remains constant, and less transmigration of adsorbate is involved. The active sites possess the same energy, and the intermolecular forces are weakened as the distance increases from the adsorption surface (Jun et al., 2020).

Equations of Langmuir model are as follows.

$$Q_e = (Q_m * K_L * C_e) / (1 + K_L * C_e) \qquad \ldots\ldots\ldots\ldots \text{(Non-Linear)} \qquad (4.11)$$

where Q_m is the maximum adsorption capacity (mg/g)

K_L is the Langmuir constant (L/mg)

$$C_e / Q_e = C_e / Q_m + 1 / (Q_m * K_L) \qquad \ldots\ldots\ldots\ldots\ldots \text{(Linear)} \qquad (4.12)$$

Q_m is determined by the slope and K_L is measured from the interaction of fitted line on abscissa (C_e) and ordinate(C_e / Q_e).

Langmuir isotherm (R_L) is also known as balance parameter or separation factor as it is a dimensionless constant having formula as follows.

$$R_L = 1 / (1 + K_L * C_i) \qquad (4.13)$$

where R_L is dimensionless constant, C_i is the initial concentration of Cr (VI) pollutant.

R_L also indicated the type of adsorption. $R_L = 1$ represents linear adsorption, $R_L > 1$ represents unfavorable adsorption, $R_L = 0$ represents irreversible adsorption, and $0 < R_L < 1$ represents favorable adsorption (Bazaine et al., 2022).

Freundlich isotherm model is related to the heterogenous surface of the adsorbent and describes the exponential behavior of the active sites and their binding energies (Fard et al., 2017).

Equations of Freundlich model are as follows.

$$Q_e = K_F + C_e^n \qquad \dots\dots\dots\dots\dots\dots\dots \text{ (Non-Linear)} \qquad (4.14)$$

K_F is the Freundlich constant (mg/g), and n represents Freundlich exponent related to the intensity of adsorption. n is dimensionless. Linearized equation of the Freundlich model is as follows

$$log\ Q_e = (1/n)\ log\ C_e + log\ K_F \dots\dots\dots\dots\dots\dots \text{ (Linear)} \qquad (4.15)$$

n is determined by the slope and K_F is determined from intercept of fitted graphical line on abscissa (lnC_e) and ordinate (lnQ_e).

The value of 1/n range from 0 to 1 and depicts the degree of non-linearity between adsorption and concentration of solution. Value of (1/n) = 1 shows linear adsorption. Lower values of n corresponds to the presence of abundant high energy active sites whereas higher values of n shows that the surface is a bit uniform in structure (Bazaine et al., 2022).

Tempkin isotherm model describes the interactions between the adsorbate and species. Equations of Tempkin model are as follows.

$$Q_e = (RT\ /\ b)\ ln(K_T * C_e) \qquad \dots\dots\dots\dots\dots\dots \text{ (Non-Linear)} \qquad (4.16)$$

where.

$$(RT\ /\ b) = B \qquad (4.17)$$

b represents Tempkin constant. K_T is for Bound Equilibrium constant (L/g) and B is referred as heat of adsorption with units J/mol. Linearized equation of the Tempkin model is as follows

$$Q_e = B\ ln\ C_e + B\ lnK_T \dots\dots\dots\dots\dots\dots\dots\dots\dots \text{(Linear)} \qquad (4.18)$$

B and K_T can be determined from slope and intersections of lines fitted by plotting Q_e on the ordinate and ln C_e on the abscissa (Bazaine et al., 2022).
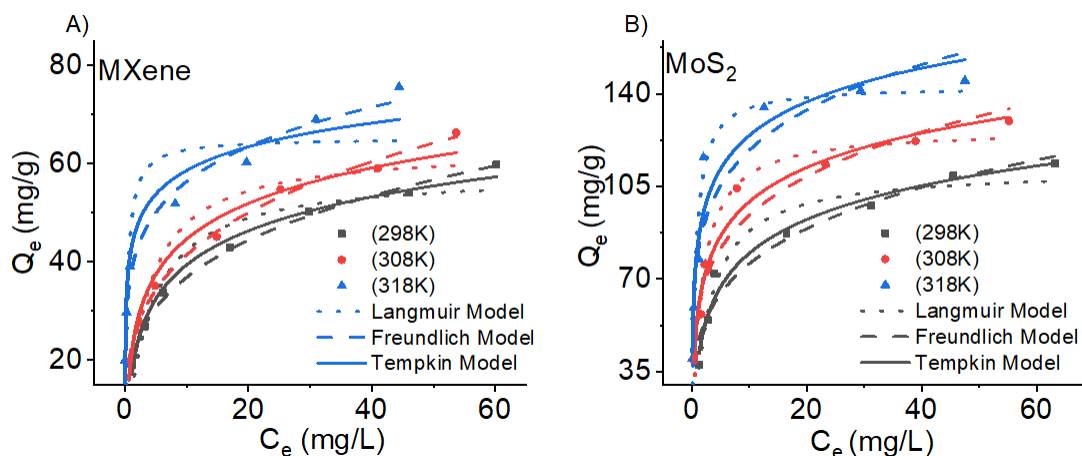
Figure 4.11: Fit of data to nonlinear isotherms of Langmuir, Freundlich and Tempkin Model (A) MXene and (B) MoS_2 at T= 298 K, 308 K, 318 K).

The fitting plots of linear Langmuir, Freundlich and Tempkin models for the removal of hexavalent chromium are shown in Figure 4.12, Figure 4.13, and Figure 4.14 for MXene and Figure 4.15, Figure 4.16, and Figure 4.17 for MoS_2 at T = 298K, 308K and 318K respectively. Also, isotherm parameters and chi square values calculated from the experimental data are shown in Table 4.4.

Table 4.4: Langmuir Freundlich and Tempkin Parameters for Cr(VI) sorption on two dimensional MXene and Molybdenum Disulphide.

Isotherm Model	Adsorbent					
	MXene T(K)			MoS_2 T(K)		
	298	308	318	298	308	318
Langmuir model Linear						
Q_m	61.88453	68.086	74.43299	117.73593	131.32983	146.28767
b (K_L)	0.20058	0.2255	0.63115	0.26277	0.4963	1.37287
R_L	0.1425	0.12879	0.05016	0.11257	0.06294	0.0237
R^2	0.98924	0.98405	0.9849	0.99427	0.99723	0.9996
Non-Linear Best fit values						
Q_m	58.08086	63.22466	65.21087	111.53312	126.60033	142.83439
b (K)	0.26746	0.31041	2.6571	0.37356	0.63843	1.6353
R^2	0.91895	0.87804	0.72407	0.94865	0.94944	0.92575
X^2	18.25742	36.49205	117.409	41.52163	61.10199	135.58129

Isotherm Model		MXene T(K)			MoS$_2$ T(K)		
	298	308	318	298	308	318
Std error						
Q$_m$	3.21786	4.5338	5.79248	4.2893	5.01873	7.1602
b(K)	0.06757	0.10378	1.5181	0.06662	0.1235	0.41746
Goodness of fit						
Degrees of freedom	5	5	5	5	5	5
Number of points Analyzed	7	7	7	7	7	7
Freundlich model Linear						
K$_F$	19.30478	22.04332	39.29928	41.2009	53.88313	73.44234
1/n	0.27815	0.27364	0.1671	0.25727	0.23827	0.21209
R^2	0.99299	0.99652	0.99137	0.91072	0.92617	0.88509
Non-linear Best fit values						
K$_F$	19.91323	22.15969	37.99446	44.27104	58.3098	79.38933
n	3.73631	3.67775	5.83374	4.28897	4.80817	5.73324
R^2	0.9939	0.99435	0.98586	0.94188	0.927	0.86545
X^2	1.37408	1.69071	6.01526	46.99017	88.21097	245.6789
Std. error						
K$_F$	0.68563	0.74259	1.25387	4.03228	5.11221	7.49695
n	0.1421	0.13788	0.36524	0.4995	0.64126	1.0602
Goodness of fit						
Degrees of freedom	5	5	5	5	5	5
Number of points Analyzed	7	7	7	7	7	7
Tempkin model Linear						
B$_T$	9.98992	10.45347	6.96347	18.46316	18.75173	18.3871
K$_T$	5.16216	7.16854	452.61265	7.4782	19.75939	85.7793
R^2	0.98693	0.96611	0.9086	0.96716	0.96725	0.9288
Nonlinear						
B$_T$	9.98992	10.45347	6.96347	18.46316	18.75173	18.3871

Isotherm Model	Adsorbent					
	MXene T(K)			MoS$_2$ T(K)		
	298	308	318	298	308	318
K$_T$	5.16216	7.16854	452.61265	7.4782	19.75939	85.7793
R^2	0.98693	0.96611	0.94086	0.96716	0.96725	0.9288

Units: Qm: mg/g, b: L/mg, K$_F$: mg/g

From table 4.4 it can be concluded that for Cr(VI) adsorption at MXene nanosheets, Freundlich linear and nonlinear isotherms had higher R^2 values as compared to linear and nonlinear Langmuir and Tempkin isotherm models. In addition to that, X^2 values of Freundlich isotherm model are lower than Langmuir isotherm model. In the case of MoS$_2$, linear and nonlinear Langmuir isotherm model had higher R^2 values as compared to linear and nonlinear Freundlich and Tempkin isotherm model. Moreover, X^2 values of Langmuir isotherm model are lower than Freundlich isotherm model. Higher values of R^2 and lower values of X^2 for isotherm models suggest the best fitting of Freundlich and Langmuir isotherm models on MXene and MoS$_2$ respectively. The maximum adsorption capacities achieved in case of both adsorbents were close to experimental values at different temperatures of 298 K, 308 K and 318 K. The fitting of Freundlich model in case of MXene suggests that process of Cr(VI) adsorption at MXene nanosheets was heterogenous adsorption and the highest adsorption capacities achieved at 298 K, 308 K and 318 K were 59.805 mg/g, 66.329 mg/g, and 75.582 mg/g respectively whereas for MoS$_2$ the best fitting of Langmuir model was observed which means that the process of Cr(VI) adsorption at MoS$_2$ was homogenous adsorption and the highest adsorption capacities achieved at 298 K, 308 K and 318 K were 113.71 mg/g, 129.68 mg/g, and 144.97 mg/g respectively. The increase in K$_f$ values with increasing temperature signifies that the adsorption capabilities improve with the rise in temperature (Xiang et al., 2021). Also, the values of other coefficients in the table such as b > 0 and 1/n (0 < 1/ n > 1) depict the rapid capture of chromium ions on MXene and MoS$_2$. R$_L$ values were also calculated to check the influence of temperature on Cr(VI) adsorption. All the R$_L$ values are falling between 0 and 1 for both adsorbents which shows that the adsorption was favorable at all the three temperatures. The data in Table 4.4 summarizes the overall performance of MXene and MoS$_2$ adsorbents for Cr(VI) removal. The comparison in both materials highlights that MoS$_2$ shows good removal efficiencies for chromium removal as compared to MXene.

Figure 4.12: Fit of data to linear isotherms of Langmuir, Freundlich and Tempkin Model MXene at T= 298 K.

Figure 4.13: Fit of data to linear isotherms of Langmuir, Freundlich and Tempkin Model MXene at T= 308 K.

Figure 4.14: Fit of data to linear isotherms of Langmuir, Freundlich and Tempkin Model MXene at T= 318 K.
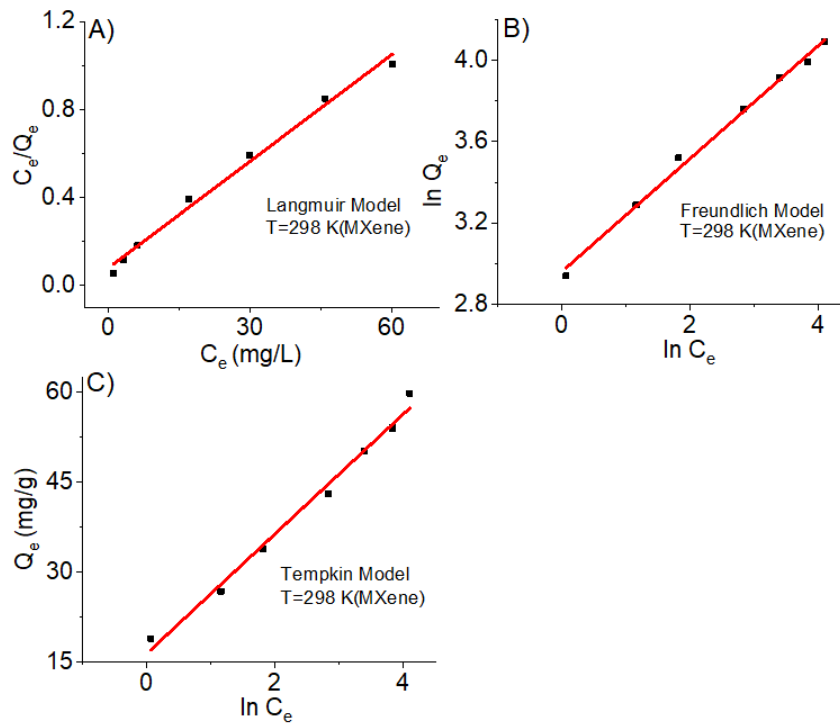

Figure 4.15: Fit of data to linear isotherms of Langmuir, Freundlich and Tempkin Model MoS$_2$ at T= 298 K.
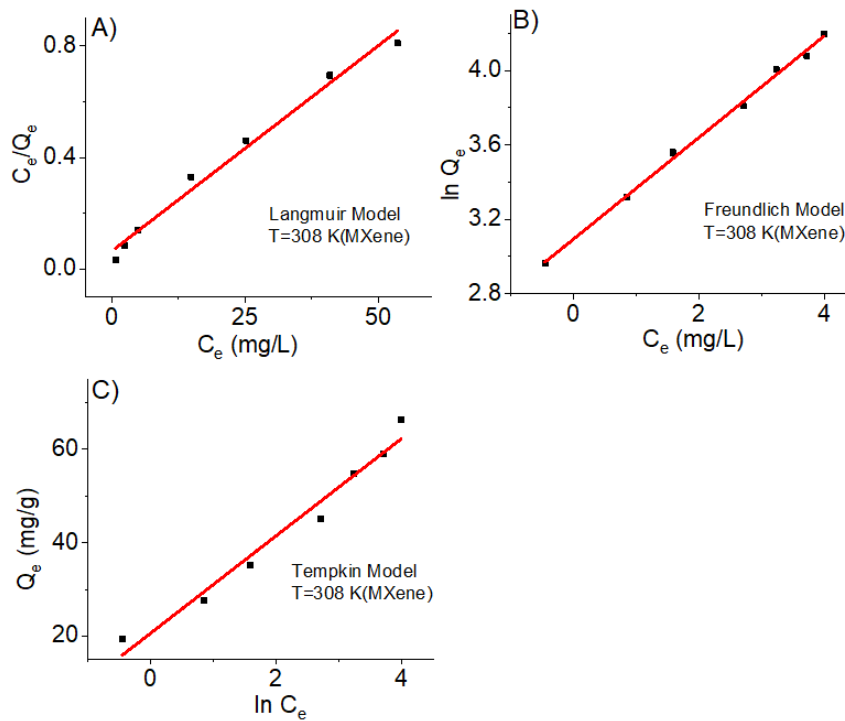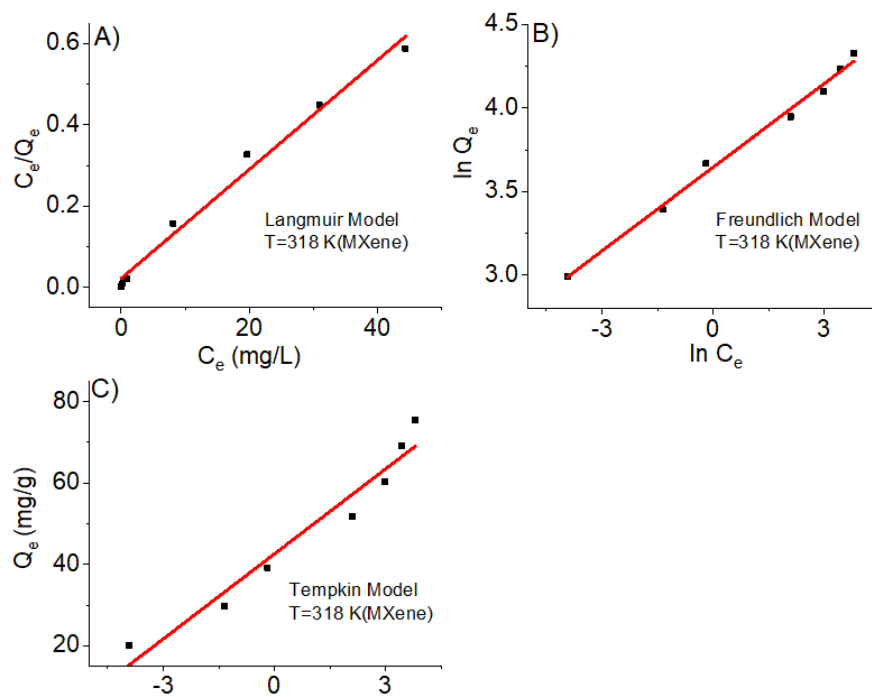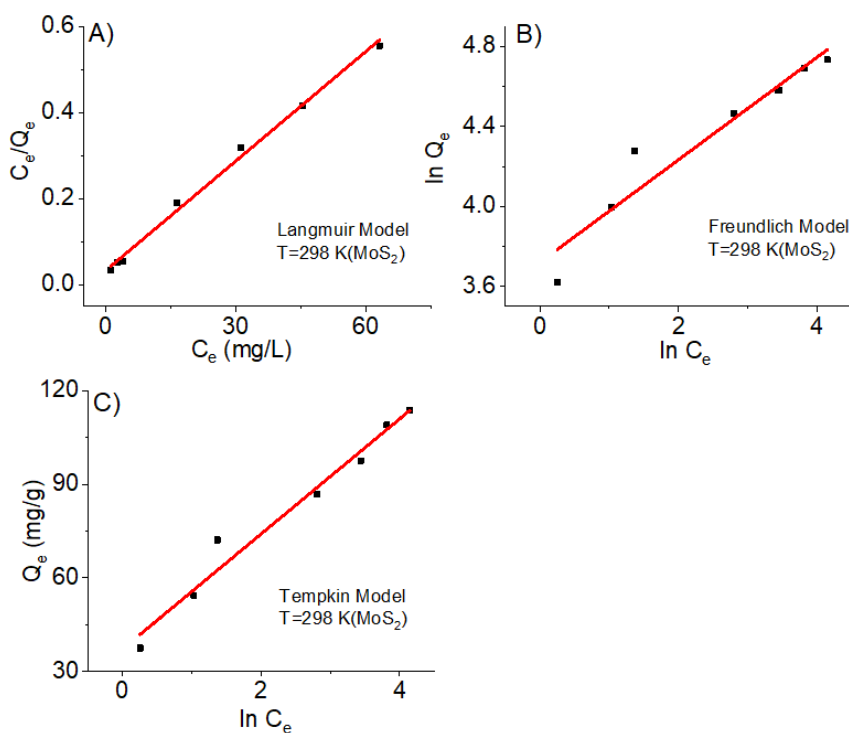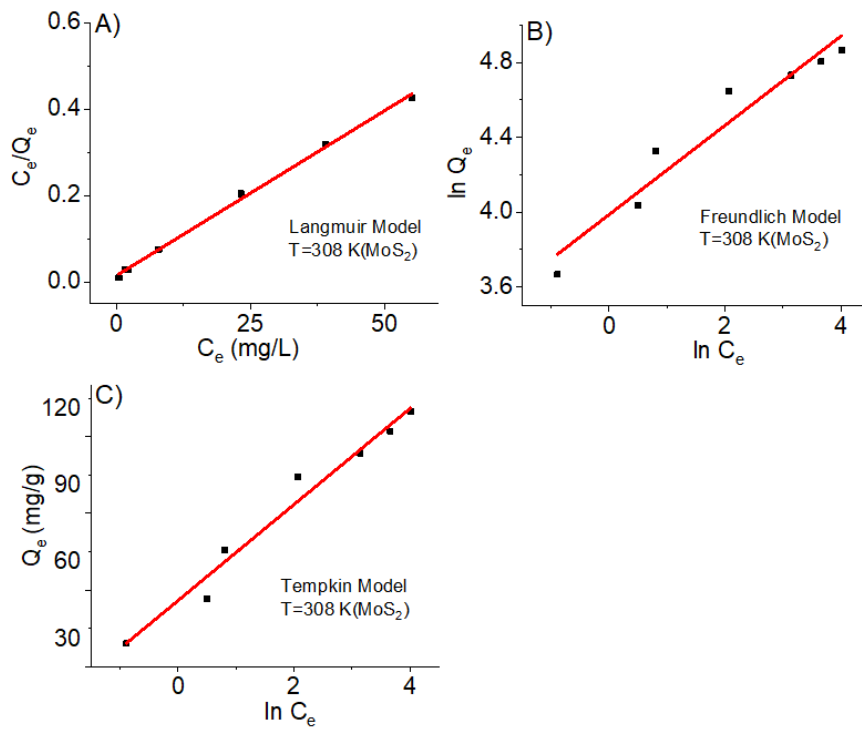
Figure 4.16: Fit of data to linear isotherms of Langmuir, Freundlich and Tempkin Model MoS$_2$ at T= 308 K.
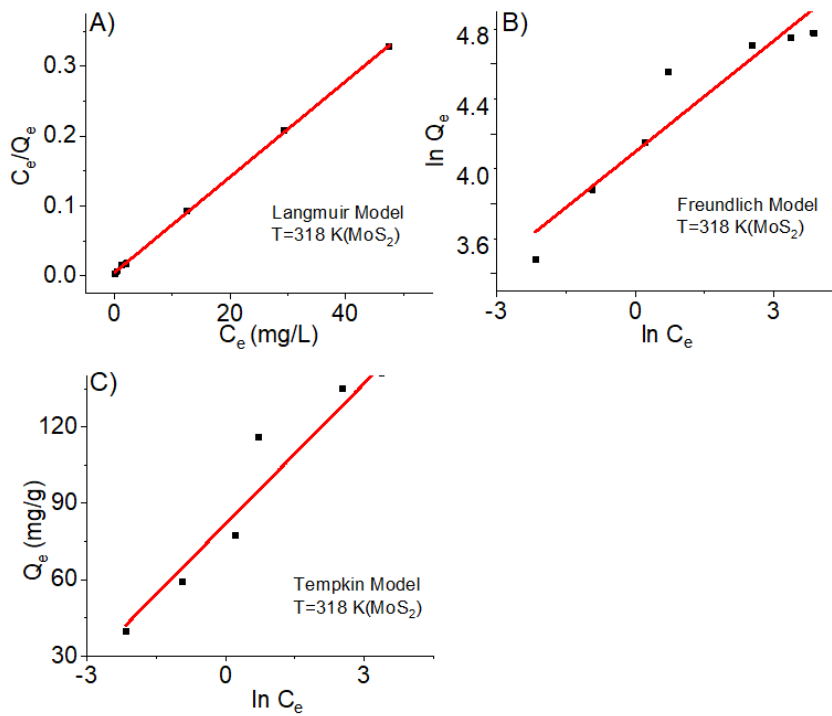
Figure 4.17: Fit of data to linear isotherms of Langmuir, Freundlich and Tempkin Model MoS$_2$ at T= 318 K.

4.6 Thermodynamic Investigation

To study the thermodynamic properties of the Cr(VI) adsorption on MXene and MoS$_2$, comparative analysis was performed at different temperatures of 298 K, 308 K and 318 K, at initial concentration of 30 mg/L and pH 2. It is worth mentioning that increase in temperature (298K, 308K, 318K) increases the adsorption capacities of Cr(VI) for both MXene (26.82 mg/g, 27.64 mg/g, 29.74 mg/g) and MoS$_2$ (54.39 mg/g, 56.69 mg/g, 59.20 mg/g) shown in Figure 4.18(A), 4.18(B). Similar adsorption patterns for Cr(VI) adsorption were shown by (Xiang et al., 2021; Shahzad et al., 2017). Thermodynamic parameters, including entropy (ΔS), enthalpy (ΔH) changes, and Gibbs free energy (ΔG), were calculated using the following equations:

$$K_c = \frac{Q_e}{C_e} \tag{4.19}$$

$$\Delta G = -RT ln K_C \tag{4.20}$$

$$ln K_c = (\Delta S / R) - (\Delta H / RT) \tag{4.21}$$

where K$_c$ stands for equilibrium gas constant, R represents the ideal gas constant equal to 8.314 J/mol/K, T stands for temperature in Kelvin, and Q$_e$ and C$_e$ are the adsorption capacity of adsorbent and chromium concentration in the effluent respectively. ΔS and ΔH are determined from intercept and slope of the graph plotted lnK$_C$ vs 1/T (Figure 4.19A and 4.19C). The Cr(VI) adsorption increases with an increase in temperature. All the ΔG (Figure 4.19B and 4.19D)
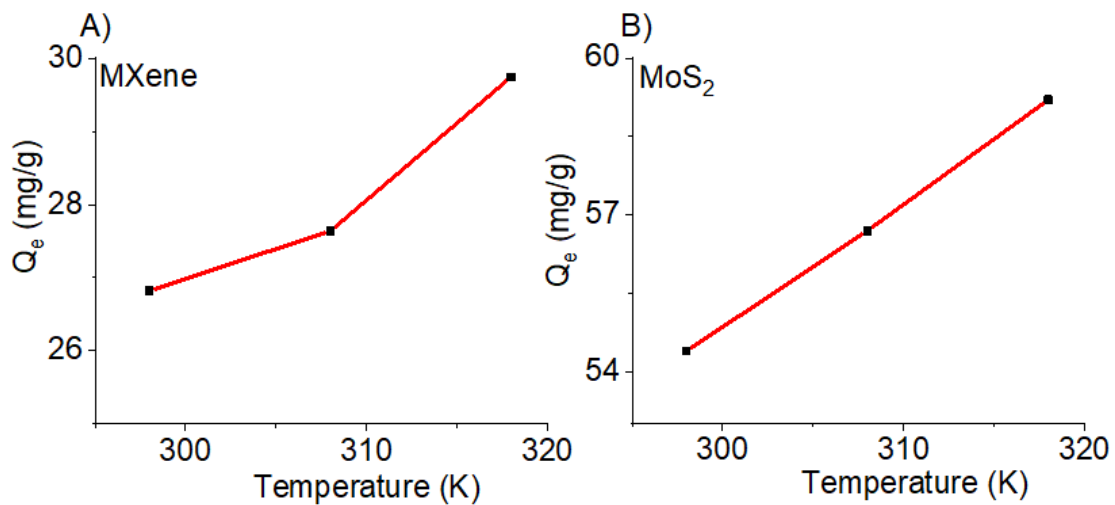
Figure 4.18: Temperature vs Adsorption Capacity (A) MXene and (B) MoS$_2$.

values are negative which indicates the reaction of adsorption was feasible and spontaneous (Xiang et al., 2021) and the decrease in ΔG with increasing temperature (Table 4.5) represents the endothermic adsorption of Cr(VI). Greater positive values of ΔH (23.46911 kJ/mol for MXene and 48.32241 kJ/mol for MoS₂) indicate that the process of adsorption on nanomaterials is endothermic and is promoted at increasing temperature. Also, the positive values of ΔS for MXene (0.06912 kJ/mol/K) and MoS₂ (0.17113 kJ/mol/K) represent high degree of dislocations and disorder at Cr(VI) / MXene and Cr(VI) /MoS₂ interface, respectively (Wang et al., 2018).
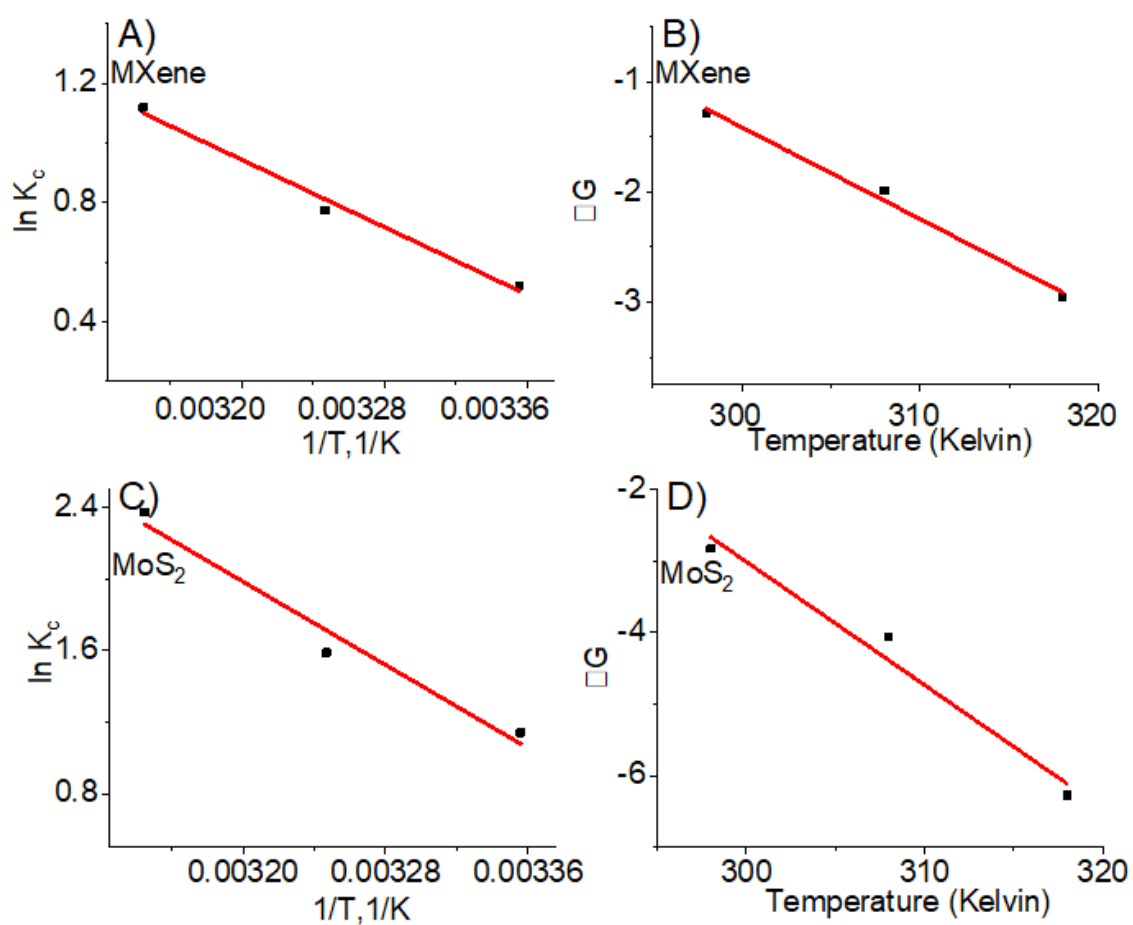
Figure 4.19: Thermodynamic parameters plot for Cr(VI) adsorption by MXene (A), (B) and by MoS₂ (C), (D).

Table 4.5: Thermodynamics parameters for Cr(VI) adsorption by MXenes and MoS$_2$.

Adsorbent	T(K)	Thermodynamic Parameters			
		ΔG	ΔH	ΔS	R^2
		(kJ/mol)	(kJ/mol)	(kJ/mol/K)	
MXene	298	-1.29194			
	308	-1.98522	23.46911	0.06912	0.978
	318	-2.95687			
MoS$_2$	298	-2.82582			
	308	-4.0661	48.32241	0.17113	0.9392
	318	-6.26934			

4.7 Effect of Coexisting Ions on Adsorption

Most of the inorganic ions are found in the drinking water (Ca^{2+}, Mg^{2+}, Na^{1+}, PO$_4^{3-}$, HCO$_3^{2-}$, Cl$^-$) and the natural water sources are contaminated due to rapid industrialization (Shahzad et al., 2020). Coexisting anions compete with Cr(VI) ions for occupying the active sites and decrease the removal percentage of Cr(VI). Therefore, to assess the efficiency of an adsorbent for selective adsorption performance, the effect of coexisting ions on Cr(VI) removal at MXene and MoS$_2$ were calculated, and the results are shown in Figure 4.20. Influence of three cations (Ca^{2+}, Mg^{2+}, Na$^+$) and three anions (PO$_4^{3-}$, HCO$_3^{2-}$, Cl$^-$) was studied on Cr(VI) removal using MXene Figure 4.15A) and MoS$_2$ (Figure 4.15B) respectively. Influence of three cations (Ca^{2+}, Mg^{2+}, Na$^+$) and three anions (PO$_4^{3-}$, HCO$_3^{2-}$, Cl$^-$) was studied on Cr(VI) removal using MXene (Figure 4.20A) and MoS$_2$ (Figure 4.20B) respectively. From the above results it can be concluded that the positive ions had little competition with Cr(VI) ions as the adsorbents were positively charged in the acidic media which favored electrostatic repulsion as compared to anions which showed more competitiveness due to the negative charge which was attracted by both adsorbents. In the case of MXenes, the competitiveness in the ability of anions for adsorption is shown maximum for PO$_4^{3-}$ then comes the Cl$^-$ and the least effect of HCO$_3^{2-}$ is seen with Cr(VI) adsorption. The greater effect by PO$_4^{3-}$ may be attributed to varying charge distribution and hydrated radii (Xiang et al., 2021). On the other hand, MoS$_2$ exhibits varying adsorption capacities with multiple ions coexisting with Cr(VI) ions in water. The effect of

coexisting ions on Cr(VI) adsorption is not very significant in the presence of MoS$_2$. The above results ensure the better selectivity of MoS$_2$ over MXene.
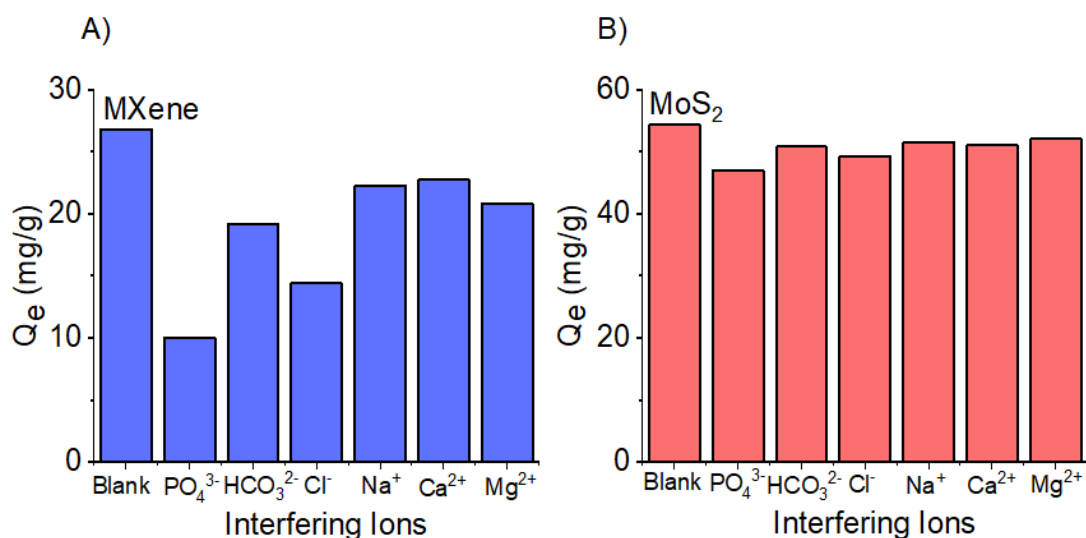
Figure 4.20: Effect of coexisting ions on Cr(VI) adsorption by (A) MXene (Dosage = 1 g/L, T = 298 K, Time = 9 h, pH = 2, C$_o$ = 30 mg/L) and (B) MoS$_2$ (Dosage = 0.5 g/L, T = 298 K, Time = 1.5 h, pH = 2, C$_o$ = 30 mg/L).

4.8 Reusability of MXenes and MoS$_2$

In order to assess the practical application of adsorbents, it is significant to evaluate the reusability and recyclability of the materials. Therefore, regeneration experiments were conducted to check if the adsorbents can be reused for the Cr(VI) removal. For experimentation, 1 g/L of MXene and 0.5 g/L of MoS$_2$ were taken in 100 ml Cr(VI) solution at room temperature with chromium concentration 30 mg/L at pH 2. Further, the materials were separated after adsorption and moved to 1 M NaOH solution. The MXene-Cr and MoS$_2$-Cr complex was agitated in 1 M NaOH solution for 8 hours to desorb the adsorbed Cr species from the surface of adsorbents. MXene and MoS$_2$ were further washed with deionized water several times to attain neutral pH for conducting the next cycle. The regenerated adsorbents were dried overnight and used again for chromium adsorption.

Figure 4.21A and Figure 4.21B show the adsorption performance of MXene and MoS$_2$ respectively, after each cycle. MXene showed a decrease in removal percentage up to 70% after fifth cycle whereas the decrease in percentage removal reached 79% in case of MoS$_2$ after fifth

51

Figure 4.21: Regeneration studies of MXenes and MoS$_2$ for Cr(VI) adsorption.

cycle. The reduction in the removal efficiencies is attributed to the loss of adsorbent's mass and the number of active sites.

CHAPTER 5: CONCLUSIONS AND RECOMMENDATIONS

5.1 Conclusions

In this study, comparison of two emerging two dimensional nanomaterials was made and MoS_2 showed efficient adsorption capacities for Cr(VI) removal as compared to MXenes. MXenes and MoS_2 were utili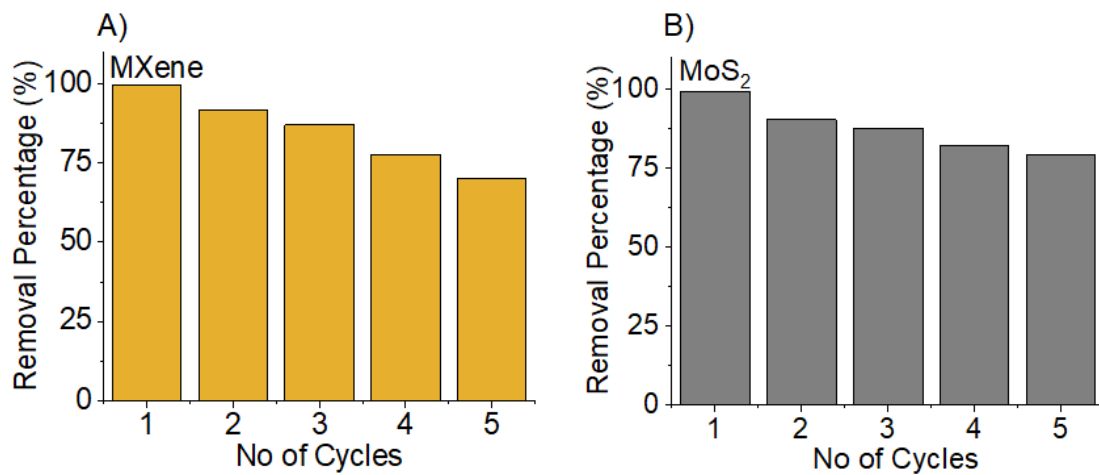zed in unmodified form to better compare both the materials in water treatment applications. MoS_2 nanosheets performed well due to the addition of PVP in synthesis process. Different characterization techniques such as SEM, XRD, FTIR and BET confirmed the successful synthesis of MXene and MoS_2. The effect of adsorption parameters was also applied on both adsorbents to better understand the operating conditions and performance operators. Both the adsorbents showed better performance as compared to the conventional adsorbents, but this needs further modification to make the process efficient and faster. The analysis of adsorption data reveals the best fit of Langmuir model for MoS_2 and Freundlich model for MXene and the maximum adsorption capacities achieved for MXene and MoS_2 were 59.805 mg/g and 113.71 mg/g at 298K respectively. Furthermore, the process of adsorption was signified by the ΔG and ΔH values. The negative values of ΔG and positive values of ΔH confirm that the ongoing adsorption of both composites was spontaneous and endothermic in nature. The comparison study is a key index to highlight the properties of two-dimensional materials in water treatment applications. MXenes are arduous to handle for adsorption as they have less stability which retards its performance for heavy metal adsorption. Moreover, the research can also be extended for comparison of other two-dimensional adsorbents and the composites of two-dimensional nanomaterials. The study will pave a way for the treatment of multiple cations and anions present in industrial wastewater. The synergetic effect of both adsorbents will be a good approach to trap the negative ions of chromium. It can be convinced that both MXene and MoS_2 are potential adsorbents for heavy metal adsorption even in unmodified form and this potential can further be enhanced through multiple approaches of modification. To the best of our knowledge, this is the first comparative study conducted for Cr(VI) removal using MXene and MoS_2 without any surface modification. The higher removal efficiencies over conventional adsorbents at different time intervals suggests that MXene and MoS_2 can further be functionalized and manipulated with desired materials to improve their performances in water and wastewater treatment applications.

5.2 Recommendations

Conventional adsorbents are less efficient in the adsorption process. Different challenges are still associated with emerging two-dimensional materials in terms of cost, their stability, preparation procedure and laboratory synthesis. It is the dire need to develop synthesis methods which require less cost and give more yield. Multiple two-dimensional materials have been discovered till now with unique chemical and physical properties. MXenes were discovered in 2011 and a lot of research is being done in water treatment applications. Currently, the application of MXenes is seen mostly in batch mode. Most of the experiments are run in the laboratory on a very small scale. The potential of MXenes for practical applications on large scale still needs to be considered especially in the water and wastewater treatment applications. Functionalization of MXenes also improves their stability which is one of the serious challenges associated to MXenes, so extended study is required to improve the stability of MXenes and improvement in the antioxidant capacity of MXenes. Studies are conducted on the treatment of a single pollutant in water treatment, but the real water treatment performed is different from the ultrapure water treated in the laboratory. The fate of MXenes in the complex water treatment needs to be studied to deal with environmental concerns.

MoS_2 nanoparticles are more favorable for the elimination of softer heavy metals over conventional adsorbents and other nanomaterials. MoS_2 nanomaterials have been widely tested and modified for multiple water treatment applications due to their extraordinary performance in the removal of pollutant ions but their use in large scale application is still a major concern mainly because of fast separation from the solution. MoS_2 nanoparticles can be made magnetic through different techniques for easy separation from solution after treatment. Also, the stability of these materials has remained a serious issue for the researchers. They easily get oxidized in some solutions which also release certain harmful ions to the solution such as . MoO_4^{2-}, SO_4^{2-}. Efforts need to be made in future to make these nanomaterials cost effective with simple and efficient process preparation methods.

REFERENCES

Abilio, T. E., Soares, B. C., Cristina José, J., Milani, P. A., Labuto, G., Neide, E., & Martins Carrilho, V. (n.d.). *Hexavalent chromium removal from water: adsorption properties of in natura and magnetic nanomodified sugarcane bagasse.* https://doi.org/10.1007/s11356-020-11726-8/Published

Adewumi, A. J. (2022). Heavy Metals in Soils and Road Dust in Akure City, Southwest Nigeria: Pollution, Sources, and Ecological and Health Risks. *Exposure and Health*, *14*(2), 375–392. https://doi.org/10.1007/s12403-021-00456-y

Ahmad, S. W., Zafar, M. S., Ahmad, S., Zia-Ul-Haq, M., Ashraf, M., Rabbani, J., & Ullah, S. (2019). Removal of Chromium(VI) from wastewater through ion exchange. Kinetic and scale up studies. *Environment Protection Engineering*, *45*(1), 17–29. https://doi.org/10.37190/epe190102

Ahmad, S. Z. N., Wan Salleh, W. N., Ismail, A. F., Yusof, N., Mohd Yusop, M. Z., & Aziz, F. (2020). Adsorptive removal of heavy metal ions using graphene-based nanomaterials: Toxicity, roles of functional groups and mechanisms. *Chemosphere*, *248*, 126008. https://doi.org/10.1016/j.chemosphere.2020.126008

Ahmed, W., Núñez-Delgado, A., Mehmood, S., Ali, S., Qaswar, M., Shakoor, A., & Chen, D. Y. (2021). Highly efficient uranium (VI) capture from aqueous solution by means of a hydroxyapatite-biochar nanocomposite: Adsorption behavior and mechanism. *Environmental Research*, *201*(April). https://doi.org/10.1016/j.envres.2021.111518

Aigbe, U. O., & Osibote, O. A. (2020). A review of hexavalent chromium removal from aqueous solutions by sorption technique using nanomaterials. *Journal of Environmental Chemical Engineering*, *8*(6), 104503. https://doi.org/10.1016/j.jece.2020.104503

Alhabeb, M., Maleski, K., Anasori, B., Lelyukh, P., Clark, L., Sin, S., & Gogotsi, Y. (2017). Guidelines for Synthesis and Processing of Two-Dimensional Titanium Carbide (Ti3C2Tx MXene). *Chemistry of Materials*, *29*(18), 7633–7644. https://doi.org/10.1021/acs.chemmater.7b02847

Ali, M. E. M., Mohammed, R., Abdel-Moniem, S. M., El-Liethy, M. A., & Ibrahim, H. S. (2022). Green MoS2 nanosheets as a promising material for decontamination of hexavalent chromium, pharmaceuticals, and microbial pathogen disinfection: spectroscopic study. *Journal of Nanoparticle Research*, *24*(10). https://doi.org/10.1007/s11051-022-05573-6

Almeida, J. C., Cardoso, C. E. D., Tavares, D. S., Freitas, R., Trindade, T., Vale, C., & Pereira, E. (2019). Chromium removal from contaminated waters using nanomaterials – A review. *TrAC - Trends in Analytical Chemistry*, *118*, 277–291. https://doi.org/10.1016/j.trac.2019.05.005

Anirudhan, T. S., & Senan, P. (2011). Adsorptive characteristics of chromium(VI) ions from aqueous phase by iron(III) coordinated amino-functionalized poly(glycidyl methacrylate)-grafted cellulose: Equilibrium kinetics and thermodynamic study. *Separation Science and Technology*, *46*(9), 1430–1442. https://doi.org/10.1080/01496395.2011.558884

Ashraf, A., Bibi, I., Niazi, N. K., Ok, Y. S., Murtaza, G., Shahid, M., Kunhikrishnan, A., Li,

D., & Mahmood, T. (2017). Chromium(VI) sorption efficiency of acid-activated banana peel over organo-montmorillonite in aqueous solutions. *International Journal of Phytoremediation*, *19*(7), 605–613. https://doi.org/10.1080/15226514.2016.1256372

Aslani, H., Ebrahimi Kosari, T., Naseri, S., Nabizadeh, R., & Khazaei, M. (2018). Hexavalent chromium removal from aqueous solution using functionalized chitosan as a novel nano-adsorbent: modeling and optimization, kinetic, isotherm, and thermodynamic studies, and toxicity testing. *Environmental Science and Pollution Research*, *25*(20), 20154–20168. https://doi.org/10.1007/s11356-018-2023-1

Astuti, R. D. P., Mallongi, A., Amiruddin, R., Hatta, M., & Rauf, A. U. (2023). Hexavalent chromium contamination in groundwater and its implication to human health: a Monte Carlo model approach in Indonesia. *Sustainable Water Resources Management*, *9*(1), 1–13. https://doi.org/10.1007/s40899-022-00806-x

Avila, M., Burks, T., Akhtar, F., Göthelid, M., Lansåker, P. C., Toprak, M. S., Muhammed, M., & Uheida, A. (2014). Surface functionalized nanofibers for the removal of chromium(VI) from aqueous solutions. *Chemical Engineering Journal*, *245*, 201–209. https://doi.org/10.1016/j.cej.2014.02.034

Baig, M. M., Pervaiz, E., Yang, M., & Gul, I. H. (2020). High-Performance Supercapacitor Electrode Obtained by Directly Bonding 2D Materials: Hierarchal MoS2 on Reduced Graphene Oxide. *Frontiers in Materials*, *7*(November), 1–12. https://doi.org/10.3389/fmats.2020.580424

Benjamin, S. E., & Nishat, M. A. (2021). Impacts of tanneries wastewater on the vicinal flora of Sheikhupura and Kasur, Pakistan. *Ovidius University Annals of Chemistry*, *32*(1), 90–97. https://doi.org/10.2478/auoc-2021-0013

Boretti, A., & Rosa, L. (2019). Reassessing the projections of the World Water Development Report. *Npj Clean Water*, *2*(1). https://doi.org/10.1038/s41545-019-0039-9

Boussouga, Y. A., Okkali, T., Luxbacher, T., & Schäfer, A. I. (2023). Chromium (III) and chromium (VI) removal and organic matter interaction with nanofiltration. *Science of the Total Environment*, *885*(April). https://doi.org/10.1016/j.scitotenv.2023.163695

Cai, W., Dionysiou, D. D., Fu, F., & Tang, B. (2020). CTAB–intercalated molybdenum disulfide nanosheets for enhanced simultaneous removal of Cr(VI) and Ni(II) from aqueous solutions. *Journal of Hazardous Materials*, *396*(April), 122728. https://doi.org/10.1016/j.jhazmat.2020.122728

Chai, W. S., Cheun, J. Y., Kumar, P. S., Mubashir, M., Majeed, Z., Banat, F., Ho, S. H., & Show, P. L. (2021). A review on conventional and novel materials towards heavy metal adsorption in wastewater treatment application. *Journal of Cleaner Production*, *296*, 126589. https://doi.org/10.1016/j.jclepro.2021.126589

Chandio, T. A., Khan, M. N., Muhammad, M. T., Yalcinkaya, O., Turan, E., & Kayis, A. F. (2021). Health risk assessment of chromium contamination in the nearby population of mining plants, situated at Balochistan, Pakistan. *Environmental Science and Pollution Research*, *28*(13), 16458–16469. https://doi.org/10.1007/s11356-020-11649-4

Chen, M., Guo, Q., Cui, J., Lv, W., & Yao, Y. (2022). Enhanced sorption and reduction of Cr(VI) by the flowerlike nanocomposites combined with molybdenum disulphide and polypyrrole. *Environmental Technology (United Kingdom)*, *43*(18), 2796–2808.

https://doi.org/10.1080/09593330.2021.1903566

de Borja Ojembarrena, F., Sammaraie, H., Campano, C., Blanco, A., Merayo, N., & Negro, C. (2022). Hexavalent Chromium Removal from Industrial Wastewater by Adsorption and Reduction onto Cationic Cellulose Nanocrystals. *Nanomaterials*, *12*(23). https://doi.org/10.3390/nano12234172

Fard, A. K., Mckay, G., Chamoun, R., Rhadfi, T., Preud'Homme, H., & Atieh, M. A. (2017). Barium removal from synthetic natural and produced water using MXene as two dimensional (2-D) nanosheet adsorbent. *Chemical Engineering Journal*, *317*, 331–342. https://doi.org/10.1016/j.cej.2017.02.090

Feng, Y., Wang, H., Xu, J., Du, X., Cheng, X., & Du, Z. (2021). Fabrication of MXene / PEI functionalized sodium alginate aerogel and its excellent adsorption behavior for Cr (VI) and Congo Red from aqueous solution. *Journal of Hazardous Materials*, *416*(April), 125777. https://doi.org/10.1016/j.jhazmat.2021.125777

Fida, M., Li, P., Wang, Y., Alam, S. M. K., & Nsabimana, A. (2023). Water Contamination and Human Health Risks in Pakistan: A Review. *Exposure and Health*, *15*(3), 619–639. https://doi.org/10.1007/s12403-022-00512-1

Geissen, V., Mol, H., Klumpp, E., Umlauf, G., Nadal, M., van der Ploeg, M., van de Zee, S. E. A. T. M., & Ritsema, C. J. (2015). Emerging pollutants in the environment: A challenge for water resource management. *International Soil and Water Conservation Research*, *3*(1), 57–65. https://doi.org/10.1016/j.iswcr.2015.03.002

Geng, J., Yin, Y., Liang, Q., Zhu, Z., & Luo, H. (2019). Polyethyleneimine cross-linked graphene oxide for removing hazardous hexavalent chromium: Adsorption performance and mechanism. *Chemical Engineering Journal*, *361*(October 2018), 1497–1510. https://doi.org/10.1016/j.cej.2018.10.141

Georgaki, M. N., & Charalambous, M. (2023). Toxic chromium in water and the effects on the human body: a systematic review. *Journal of Water and Health*, *21*(2), 205–223. https://doi.org/10.2166/wh.2022.214

Georgaki, M. N., Charalambous, M., Kazakis, N., Talias, M. A., Georgakis, C., Papamitsou, T., & Mytiglaki, C. (2023). Chromium in Water and Carcinogenic Human Health Risk. *Environments - MDPI*, *10*(2), 1–26. https://doi.org/10.3390/environments10020033

Ghernaout, D. (2015). Controlling Coagulation Process: From Zeta Potential to Streaming Potential. *American Journal of Environmental Protection*, *4*(5), 16. https://doi.org/10.11648/j.ajeps.s.2015040501.12

Hairom, N. H. H., Soon, C. F., Mohamed, R. M. S. R., Morsin, M., Zainal, N., Nayan, N., Zulkifli, C. Z., & Harun, N. H. (2021). A review of nanotechnological applications to detect and control surface water pollution. *Environmental Technology and Innovation*, *24*, 102032. https://doi.org/10.1016/j.eti.2021.102032

Harijan, D. K. L., & Chandra, V. (2016). Polyaniline functionalized graphene sheets for treatment of toxic hexavalent chromium. *Journal of Environmental Chemical Engineering*, *4*(3), 3006–3012. https://doi.org/10.1016/j.jece.2016.06.014

He, L., Huang, D., He, Z., Yang, X., Yue, G., Zhu, J., Astruc, D., & Zhao, P. (2020). Nanoscale zero-valent iron intercalated 2D titanium carbides for removal of Cr(VI) in aqueous

solution and the mechanistic aspect. *Journal of Hazardous Materials*, *388*(June 2019), 121761. https://doi.org/10.1016/j.jhazmat.2019.121761

He, X., & Li, P. (2020). Surface Water Pollution in the Middle Chinese Loess Plateau with Special Focus on Hexavalent Chromium (Cr6+): Occurrence, Sources and Health Risks. *Exposure and Health*, *12*(3), 385–401. https://doi.org/10.1007/s12403-020-00344-x

Heidari, A., Sayadi, M. H., & Biglari Quchan Atigh, Z. (2021). A comparative study of different materials (drinking water treatment sludge, nanoclay, and modified nanoclay) for simultaneous removal of hexavalent chromium and lead. *International Journal of Environmental Science and Technology*, *18*(11), 3553–3570. https://doi.org/10.1007/s13762-020-03074-4

Hiller, M. M., & Leggett, R. W. (2020). A biokinetic model for trivalent or hexavalent chromium in adult humans. *Journal of Radiological Protection*, *40*(1), 19–39. https://doi.org/10.1088/1361-6498/ab4286

Ihsanullah, I. (2020). MXenes (two-dimensional metal carbides) as emerging nanomaterials for water purification: Progress, challenges and prospects. *Chemical Engineering Journal*, *388*(December 2019), 124340. https://doi.org/10.1016/j.cej.2020.124340

Inobeme, A., Mathew, J. T., Adetunji, C. O., Ajai, A. I., Inobeme, J., Maliki, M., Okonkwo, S., Adekoya, M. A., Bamigboye, M. O., Jacob, J. O., & Eziukwu, C. A. (2023). Recent advances in nanotechnology for remediation of heavy metals. *Environmental Monitoring and Assessment*, *195*(1). https://doi.org/10.1007/s10661-022-10614-7

Jamaluddin, N. S., Alias, N. H., Samitsu, S., Othman, N. H., Jaafar, J., Marpani, F., Lau, W. J., & Tan, Y. Z. (2022). Efficient chromium (VI) removal from wastewater by adsorption-assisted photocatalysis using MXene. *Journal of Environmental Chemical Engineering*, *10*(6), 108665. https://doi.org/10.1016/j.jece.2022.108665

Jiang, X., Luo, H., Yin, Y., & Zhou, W. (2017). Facile synthesis of MoS2/reduced graphene oxide composites for efficient removal of Cr(VI) from aqueous solutions. *RSC Advances*, *7*(39), 24149–24156. https://doi.org/10.1039/c7ra03531d

Jin, L., Chai, L., Ren, L., Jiang, Y., Yang, W., Wang, S., Liao, Q., Wang, H., & Zhang, L. (2019). Enhanced adsorption-coupled reduction of hexavalent chromium by 2D poly(m-phenylenediamine)-functionalized reduction graphene oxide. *Environmental Science and Pollution Research*, *26*(30), 31099–31110. https://doi.org/10.1007/s11356-019-06175-x

Jin, L., Chai, L., Yang, W., Wang, H., & Zhang, L. (2020). Two-dimensional titanium carbides (Ti3 C2 Tx) functionalized by poly(m-phenylenediamine) for efficient adsorption and reduction of hexavalent chromium. *International Journal of Environmental Research and Public Health*, *17*(1). https://doi.org/10.3390/ijerph17010167

Jun, B. M., Heo, J., Taheri-Qazvini, N., Park, C. M., & Yoon, Y. (2020). Adsorption of selected dyes on Ti3C2Tx MXene and Al-based metal-organic framework. *Ceramics International*, *46*(3), 2960–2968. https://doi.org/10.1016/j.ceramint.2019.09.293

Karthikeyan, P., Elanchezhiyan, S. S. D., Banu, H. A. T., Hasmath Farzana, M., & Park, C. M. (2021). Hydrothermal synthesis of hydroxyapatite-reduced graphene oxide (1D–2D) hybrids with enhanced selective adsorption properties for methyl orange and hexavalent chromium from aqueous solutions. *Chemosphere*, *276*, 130200. https://doi.org/10.1016/j.chemosphere.2021.130200

Karthikeyan, P., Elanchezhiyan, S. S. D., Preethi, J., Meenakshi, S., & Park, C. M. (2020). Mechanistic performance of polyaniline-substituted hexagonal boron nitride composite as a highly efficient adsorbent for the removal of phosphate, nitrate, and hexavalent chromium ions from an aqueous environment. *Applied Surface Science*, *511*(January), 145543. https://doi.org/10.1016/j.apsusc.2020.145543

Karthikeyan, P., Ramkumar, K., Pandi, K., Fayyaz, A., Meenakshi, S., & Park, C. M. (2021). Effective removal of Cr(VI) and methyl orange from the aqueous environment using two-dimensional (2D) Ti3C2Tx MXene nanosheets. *Ceramics International*, *47*(3), 3692–3698. https://doi.org/10.1016/j.ceramint.2020.09.221

Kekes, T., Kolliopoulos, G., & Tzia, C. (2021). Hexavalent chromium adsorption onto crosslinked chitosan and chitosan/β-cyclodextrin beads: Novel materials for water decontamination. *Journal of Environmental Chemical Engineering*, *9*(4), 105581. https://doi.org/10.1016/j.jece.2021.105581

Kerur, S. S., Bandekar, S., Hanagadakar, M. S., Nandi, S. S., Ratnamala, G. M., & Hegde, P. G. (2020). Removal of hexavalent Chromium-Industry treated water and Wastewater: A review. *Materials Today: Proceedings*, *42*, 1112–1121. https://doi.org/10.1016/j.matpr.2020.12.492

Khan, S. T., & Malik, A. (2019). Engineered nanomaterials for water decontamination and purification: From lab to products. *Journal of Hazardous Materials*, *363*(October 2018), 295–308. https://doi.org/10.1016/j.jhazmat.2018.09.091

Khurshid, H., Mustafa, M. R. U., & Isa, M. H. (2022). Adsorption of chromium, copper, lead and mercury ions from aqueous solution using bio and nano adsorbents: A review of recent trends in the application of AC, BC, nZVI and MXene. *Environmental Research*, *212*(PA), 113138. https://doi.org/10.1016/j.envres.2022.113138

Kirti Shekhawat, Sreemoyee Chatterjee, B. J. (2015). Chromium toxicity and its health hazards. *International Journal of Advanced Research*, *3*(July 2015), 167.

Kong, A., Sun, Y., Peng, M., Gu, H., Fu, Y., Zhang, J., & Li, W. (2021). Amino-functionalized MXenes for efficient removal of Cr(VI). *Colloids and Surfaces A: Physicochemical and Engineering Aspects*, *617*(January), 126388. https://doi.org/10.1016/j.colsurfa.2021.126388

Konradt, N., Dillmann, S., Becker, J., Schroden, D., Rohns, H. P., Wagner, C., Müller, U., Konradt, D., Janknecht, P., Hobby, R., ElSherbiny, I. M. A., & Panglisch, S. (2023). Removal of Chromium Species from Low-Contaminated Raw Water by Different Drinking Water Treatment Processes. *Water (Switzerland)*, *15*(3). https://doi.org/10.3390/w15030516

Kumar, V., & Dwivedi, S. K. (2021). A review on accessible techniques for removal of hexavalent Chromium and divalent Nickel from industrial wastewater: Recent research and future outlook. *Journal of Cleaner Production*, *295*, 126229. https://doi.org/10.1016/j.jclepro.2021.126229

Kurniasari, F., Htike, M. T., Tazaki, A., Kagawa, T., Al Hossain, M. M. A., Akhand, A. A., Ahsan, N., Ohnuma, S., Iwasaki, N., & Kato, M. (2024). Beneficial and adverse effects of dam construction in canal tannery wastewater effluent with a high content of chromium in Hazaribagh, Bangladesh. *Chemosphere*, *350*(December 2023), 141047. https://doi.org/10.1016/j.chemosphere.2023.141047

Liu, C., Wang, Q., Jia, F., & Song, S. (2019). Adsorption of heavy metals on molybdenum disulfide in water: A critical review. *Journal of Molecular Liquids*, *292*, 111390. https://doi.org/10.1016/j.molliq.2019.111390

Liu, S., Gao, J., Zhang, L., Yang, Y., & Liu, X. (2021). Diethylenetriaminepentaacetic acid–thiourea-modified magnetic chitosan for adsorption of hexavalent chromium from aqueous solutions. *Carbohydrate Polymers*, *274*(92), 118555. https://doi.org/10.1016/j.carbpol.2021.118555

Liu, X., Ma, R., Wang, X., Ma, Y., Yang, Y., Zhuang, L., Zhang, S., Jehan, R., Chen, J., & Wang, X. (2019). Graphene oxide-based materials for efficient removal of heavy metal ions from aqueous solution: A review. *Environmental Pollution*, *252*, 62–73. https://doi.org/10.1016/j.envpol.2019.05.050

Lukina, A. O., Boutin, C., Rowland, O., & Carpenter, D. J. (2016). Evaluating trivalent chromium toxicity on wild terrestrial and wetland plants. *Chemosphere*, *162*, 355–364. https://doi.org/10.1016/j.chemosphere.2016.07.055

Lyu, H., Tang, J., Huang, Y., Gai, L., Zeng, E. Y., Liber, K., & Gong, Y. (2017). Removal of hexavalent chromium from aqueous solutions by a novel biochar supported nanoscale iron sulfide composite. *Chemical Engineering Journal*, *322*, 516–524. https://doi.org/10.1016/j.cej.2017.04.058

Maftouh, A., El Fatni, O., El Hajjaji, S., Jawish, M. W., & Sillanpää, M. (2023). Comparative Review of Different Adsorption Techniques Used in Heavy Metals Removal in Water. *Biointerface Research in Applied Chemistry*, *13*(4). https://doi.org/10.33263/BRIAC134.397

Mehmood, S., Mahmood, M., Núñez-Delgado, A., Alatalo, J. M., Elrys, A. S., Rizwan, M., Weng, J., Li, W., & Ahmed, W. (2022). A green method for removing chromium (VI) from aqueous systems using novel silicon nanoparticles: Adsorption and interaction mechanisms. *Environmental Research*, *213*(June). https://doi.org/10.1016/j.envres.2022.113614

Mohanapriya, V., Sakthivel, R., Pham, N. D. K., Cheng, C. K., Le, H. S., & Dong, T. M. H. (2023). Nanotechnology- A ray of hope for heavy metals removal. *Chemosphere*, *311*(P1), 136989. https://doi.org/10.1016/j.chemosphere.2022.136989

Mohanty, S., Benya, A., Hota, S., Kumar, M. S., & Singh, S. (2023). Eco-toxicity of hexavalent chromium and its adverse impact on environment and human health in Sukinda Valley of India: A review on pollution and prevention strategies. *Environmental Chemistry and Ecotoxicology*, *5*(November 2022), 46–54. https://doi.org/10.1016/j.enceco.2023.01.002

Mouloua, D., Kotbi, A., Deokar, G., Kaja, K., El Marssi, M., El Khakani, M. A., & Jouiad, M. (2021). Recent progress in the synthesis of MoS2 thin films for sensing, photovoltaic and plasmonic applications: A review. *Materials*, *14*(12). https://doi.org/10.3390/ma14123283

Nawab, J., Khan, S., Ali, S., Sher, H., Rahman, Z., Khan, K., Tang, J., & Ahmad, A. (2016). Health risk assessment of heavy metals and bacterial contamination in drinking water sources: a case study of Malakand Agency, Pakistan. *Environmental Monitoring and Assessment*, *188*(5). https://doi.org/10.1007/s10661-016-5296-1

Neelam, A. (2018). Determination of Chromium in the Tannery wastewater, Korangi, Karachi. *International Journal of Environmental Sciences & Natural Resources*, *15*(4). https://doi.org/10.19080/ijesnr.2018.15.555920

Peng, H., & Guo, J. (2020). Removal of chromium from wastewater by membrane filtration, chemical precipitation, ion exchange, adsorption electrocoagulation, electrochemical reduction, electrodialysis, electrodeionization, photocatalysis and nanotechnology: a review. *Environmental Chemistry Letters*, *18*(6), 2055–2068. https://doi.org/10.1007/s10311-020-01058-x

Peng, W., Li, H., Liu, Y., & Song, S. (2017). A review on heavy metal ions adsorption from water by graphene oxide and its composites. *Journal of Molecular Liquids*, *230*, 496–504. https://doi.org/10.1016/j.molliq.2017.01.064

Periyasamy, S., & Viswanathan, N. (2018). Hydrothermal synthesis of hydrocalumite assisted biopolymeric hybrid composites for efficient Cr(VI) removal from water. *New Journal of Chemistry*, *42*(5), 3371–3382. https://doi.org/10.1039/c7nj04524g

Petrinic, I., Korenak, J., Povodnik, D., & Hélix-Nielsen, C. (2015). A feasibility study of ultrafiltration/reverse osmosis (UF/RO)-based wastewater treatment and reuse in the metal finishing industry. *Journal of Cleaner Production*, *101*, 292–300. https://doi.org/10.1016/j.jclepro.2015.04.022

Prasad, S., Yadav, K. K., Kumar, S., Gupta, N., Cabral-Pinto, M. M. S., Rezania, S., Radwan, N., & Alam, J. (2021). Chromium contamination and effect on environmental health and its remediation: A sustainable approaches. *Journal of Environmental Management*, *285*(August 2020), 112174. https://doi.org/10.1016/j.jenvman.2021.112174

Prokkola, H., Nurmesniemi, E. T., & Lassi, U. (2020). Removal of metals by sulphide precipitation using na2s and hs−-solution. *ChemEngineering*, *4*(3), 1–10. https://doi.org/10.3390/chemengineering4030051

Ramli, N. N., Kurniawan, S. B., Ighalo, J. O., Mohd Said, N. S., Marsidi, N., Buhari, J., Ramli Shah, R. A., Zulkifli, M., Alias, J., Daud, N. M., Ahmad, J., Othman, A. R., Sheikh Abdullah, S. R., & Abu Hasan, H. (2023). A review of the treatment technologies for hexavalent chromium contaminated water. In *BioMetals* (Vol. 36, Issue 6). Springer Netherlands. https://doi.org/10.1007/s10534-023-00512-x

Riaz, A., & Zia, A. (2020). Appraisal of Chromium Contents from Different Tanneries and Drains of Sialkot. *Pakistan Journal of Scientific and Industrial Research Series A: Physical Sciences*, *63*(2), 112–117. https://doi.org/10.52763/pjsir.phys.sci.63.2.2020.112.117

Salleh, M. A. M., Mahmoud, D. K., Karim, W. A. W. A., & Idris, A. (2011). Cationic and anionic dye adsorption by agricultural solid wastes: A comprehensive review. *Desalination*, *280*(1–3), 1–13. https://doi.org/10.1016/j.desal.2011.07.019

Santhosh, C., Velmurugan, V., Jacob, G., Jeong, S. K., Grace, A. N., & Bhatnagar, A. (2016). Role of nanomaterials in water treatment applications: A review. *Chemical Engineering Journal*, *306*, 1116–1137. https://doi.org/10.1016/j.cej.2016.08.053

Shahid, M., Shamshad, S., Rafiq, M., Khalid, S., Bibi, I., Niazi, N. K., Dumat, C., & Rashid, M. I. (2017). Chromium speciation, bioavailability, uptake, toxicity and detoxification in soil-plant system: A review. *Chemosphere*, *178*, 513–533.

https://doi.org/10.1016/j.chemosphere.2017.03.074

Shahzad, A., Jang, J., Lim, S. R., & Lee, D. S. (2020). Unique selectivity and rapid uptake of molybdenum-disulfide-functionalized MXene nanocomposite for mercury adsorption. *Environmental Research*, *182*(September 2019), 109005. https://doi.org/10.1016/j.envres.2019.109005

Shahzad, A., Nawaz, M., Moztahida, M., Jang, J., Tahir, K., Kim, J., Lim, Y., Vassiliadis, V. S., Woo, S. H., & Lee, D. S. (2019). Ti3C2Tx MXene core-shell spheres for ultrahigh removal of mercuric ions. *Chemical Engineering Journal*, *368*(February), 400–408. https://doi.org/10.1016/j.cej.2019.02.160

Shahzad, A., Rasool, K., Miran, W., Nawaz, M., Jang, J., Mahmoud, K. A., & Lee, D. S. (2017). Two-Dimensional Ti3C2Tx MXene Nanosheets for Efficient Copper Removal from Water. *ACS Sustainable Chemistry and Engineering*, *5*(12), 11481–11488. https://doi.org/10.1021/acssuschemeng.7b02695

Shakil, S., Abbasi, N. A., Shakoor, M. B., Ahmad, S. R., Majid, M., Ali, A., & Farwa, U. (2023). Assessment of physicochemical parameters and trace elements in tannery wastewater treatment facility and associated health risks. *International Journal of Environmental Science and Technology*, *20*(10), 11287–11300. https://doi.org/10.1007/s13762-022-04737-0

Sharma, P., Bihari, V., Agarwal, S. K., Verma, V., Kesavachandran, C. N., Pangtey, B. S., Mathur, N., Singh, K. P., Srivastava, M., & Goel, S. K. (2012). Groundwater Contaminated with Hexavalent Chromium [Cr (VI)]: A Health Survey and Clinical Examination of Community Inhabitants (Kanpur, India). *PLoS ONE*, *7*(10), 3–9. https://doi.org/10.1371/journal.pone.0047877

Sheth, Y., Dharaskar, S., Chaudhary, V., Khalid, M., & Walvekar, R. (2022). Prospects of titanium carbide-based MXene in heavy metal ion and radionuclide adsorption for wastewater remediation: A review. *Chemosphere*, *293*(August 2021), 133563. https://doi.org/10.1016/j.chemosphere.2022.133563

Singh, S., Anil, A. G., Khasnabis, S., Kumar, V., Nath, B., Adiga, V., Kumar Naik, T. S. S., Subramanian, S., Kumar, V., Singh, J., & Ramamurthy, P. C. (2022). Sustainable removal of Cr(VI) using graphene oxide-zinc oxide nanohybrid: Adsorption kinetics, isotherms and thermodynamics. *Environmental Research*, *203*(April 2021), 111891. https://doi.org/10.1016/j.envres.2021.111891

Sun, H., Wu, T., Zhang, Y., Ng, D. H. L., & Wang, G. (2018). Structure-enhanced removal of Cr(vi) in aqueous solutions using MoS2 ultrathin nanosheets. *New Journal of Chemistry*, *42*(11), 9006–9015. https://doi.org/10.1039/c8nj01062e

Tang, M. S., Chen, J. H., Wang, J. M., Lin, Q. J., & Fang, L. J. (2021). *Preparation of polyethyleneimine modification of flower molybdenum disulfide composite (PEI / MoS 2) adsorbent and studying it enriched and reduction property for hexavalent chromium from wastewater*. 1–25.

Tran, H. N., Nguyen, D. T., Le, G. T., Tomul, F., Lima, E. C., Woo, S. H., Sarmah, A. K., Nguyen, H. Q., Nguyen, P. T., Nguyen, D. D., Nguyen, T. V., Vigneswaran, S., Vo, D. V. N., & Chao, H. P. (2019). Adsorption mechanism of hexavalent chromium onto layered double hydroxides-based adsorbents: A systematic in-depth review. *Journal of Hazardous Materials*, *373*(October 2018), 258–270. https://doi.org/10.1016/j.jhazmat.2019.03.018

Ukhurebor, K. E., Aigbe, U. O., Onyancha, R. B., Nwankwo, W., Osibote, O. A., Paumo, H. K., Ama, O. M., Adetunji, C. O., & Siloko, I. U. (2021). Effect of hexavalent chromium on the environment and removal techniques: A review. *Journal of Environmental Management*, *280*(September 2020), 111809. https://doi.org/10.1016/j.jenvman.2020.111809

Unesco. (2015). *Informe Mundial de las Naciones Unidas sobre el Desarrollo de los Recursos Hídricos 2015: Water for a Sustanible World*. https://unesdoc.unesco.org/ark:/48223/pf0000367303_por

Usmani, W., Inam, M. A., Iftikhar, R., Irfan, I., Adnan, R., Niazi, M. B. K., Khan, R., & Hassan, M. (2023). Efficient removal of hexavalent chromium Cr (VI) using magnesium-iron layered double hydroxide supported on orange peel (Mg-Fe LDH@OPP): A synthetic experimental and mechanism studies. *Journal of Water Process Engineering*, *55*(August), 104233. https://doi.org/10.1016/j.jwpe.2023.104233

Vaiopoulou, E., & Gikas, P. (2020). Regulations for chromium emissions to the aquatic environment in Europe and elsewhere. *Chemosphere*, *254*, 126876. https://doi.org/10.1016/j.chemosphere.2020.126876

Vilela, P. B., Dalalibera, A., Duminelli, E. C., Becegato, V. A., & Paulino, A. T. (2019). Adsorption and removal of chromium (VI) contained in aqueous solutions using a chitosan-based hydrogel. *Environmental Science and Pollution Research*, *26*(28), 28481–28489. https://doi.org/10.1007/s11356-018-3208-3

Wan, H., Nan, L., Geng, H., Zhang, W., & Shi, H. (2021). Green synthesis of a novel mxene–cs composite applied in treatment of cr(Vi) contaminated aqueous solution. *Processes*, *9*(3). https://doi.org/10.3390/pr9030524

Wang, H., Cui, H., Song, X., Xu, R., Wei, N., Tian, J., & Niu, H. (2020). Facile synthesis of heterojunction of MXenes/TiO2 nanoparticles towards enhanced hexavalent chromium removal. *Journal of Colloid and Interface Science*, *561*, 46–57. https://doi.org/10.1016/j.jcis.2019.11.120

Wang, H., Wu, F., Wang, Z., Wang, Y., Zhang, S., Luo, H., Zheng, Z., & Fang, L. (2022). Ultra-fast and ultra-efficient removal of Cr (VI) by the aqueous solutions of monolayer MXene (Ti3C2Tx). *Chemosphere*, *308*(P3), 136573. https://doi.org/10.1016/j.chemosphere.2022.136573

Wang, J., Wang, X., Zhao, G., Song, G., Chen, D., Chen, H., Xie, J., Hayat, T., Alsaedi, A., & Wang, X. (2018). Polyvinylpyrrolidone and polyacrylamide intercalated molybdenum disulfide as adsorbents for enhanced removal of chromium(VI) from aqueous solutions. *Chemical Engineering Journal*, *334*(September 2017), 569–578. https://doi.org/10.1016/j.cej.2017.10.068

Wang, Z., Sim, A., Urban, J. J., & Mi, B. (2018). Removal and Recovery of Heavy Metal Ions by Two-dimensional MoS2 Nanosheets: Performance and Mechanisms. *Environmental Science and Technology*, *52*(17), 9741–9748. https://doi.org/10.1021/acs.est.8b01705

Wang, Z., Von Dem Bussche, A., Qiu, Y., Valentin, T. M., Gion, K., Kane, A. B., & Hurt, R. H. (2016). Chemical Dissolution Pathways of MoS2 Nanosheets in Biological and Environmental Media. *Environmental Science and Technology*, *50*(13), 7208–7217. https://doi.org/10.1021/acs.est.6b01881

Wang, Z., Zhu, W., Qiu, Y., Yi, X., Von Dem Bussche, A., Kane, A., Gao, H., Koski, K., & Hurt, R. (2016). Biological and environmental interactions of emerging two-dimensional nanomaterials. *Chemical Society Reviews*, *45*(6), 1750–1780. https://doi.org/10.1039/c5cs00914f

White, R. L., White, C. M., Turgut, H., Massoud, A., & Tian, Z. R. (2018). Comparative studies on copper adsorption by graphene oxide and functionalized graphene oxide nanoparticles. *Journal of the Taiwan Institute of Chemical Engineers*, *85*, 18–28. https://doi.org/10.1016/j.jtice.2018.01.036

Xiang, L., Niu, C. G., Tang, N., Lv, X. X., Guo, H., Li, Z. W., Liu, H. Y., Lin, L. S., Yang, Y. Y., & Liang, C. (2021). Polypyrrole coated molybdenum disulfide composites as adsorbent for enhanced removal of Cr(VI) in aqueous solutions by adsorption combined with reduction. *Chemical Engineering Journal*, *408*(August 2020), 127281. https://doi.org/10.1016/j.cej.2020.127281

Xu, J., Cao, Z., Zhang, Y., Yuan, Z., Lou, Z., Xu, X., & Wang, X. (2018). A review of functionalized carbon nanotubes and graphene for heavy metal adsorption from water: Preparation, application, and mechanism. *Chemosphere*, *195*, 351–364. https://doi.org/10.1016/j.chemosphere.2017.12.061

Yang, G., Hu, X., Liang, J., Huang, Q., Dou, J., Tian, J., Deng, F., Liu, M., Zhang, X., & Wei, Y. (2021). Surface functionalization of MXene with chitosan through in-situ formation of polyimidazoles and its adsorption properties. *Journal of Hazardous Materials*, *419*(December 2020), 126220. https://doi.org/10.1016/j.jhazmat.2021.126220

Yang, W., Song, W., Li, J., & Zhang, X. (2020). Bioleaching of heavy metals from wastewater sludge with the aim of land application. *Chemosphere*, *249*. https://doi.org/10.1016/j.chemosphere.2020.126134

Yao, Y., Mi, N., He, C., Zhang, Y., Yin, L., Li, J., Wang, W., Yang, S., He, H., Li, S., & Ni, L. (2020). A novel colloid composited with polyacrylate and nano ferrous sulfide and its efficiency and mechanism of removal of Cr(VI) from Water. *Journal of Hazardous Materials*, *399*(June). https://doi.org/10.1016/j.jhazmat.2020.123082

Younas, F., Bibi, I., Afzal, M., Al-Misned, F., Niazi, N. K., Hussain, K., Shahid, M., Shakil, Q., Ali, F., & Wang, H. (2023). Unveiling Distribution, Hydrogeochemical Behavior and Environmental Risk of Chromium in Tannery Wastewater. *Water (Switzerland)*, *15*(3). https://doi.org/10.3390/w15030391

Younas, F., Niazi, N. K., Bibi, I., Afzal, M., Hussain, K., Shahid, M., Aslam, Z., Bashir, S., Hussain, M. M., & Bundschuh, J. (2022). Constructed wetlands as a sustainable technology for wastewater treatment with emphasis on chromium-rich tannery wastewater. *Journal of Hazardous Materials*, *422*(August 2021), 126926. https://doi.org/10.1016/j.jhazmat.2021.126926

Yu, G., Lu, Y., Guo, J., Patel, M., Bafana, A., Wang, X., Qiu, B., Jeffryes, C., Wei, S., Guo, Z., & Wujcik, E. K. (2018). Carbon nanotubes, graphene, and their derivatives for heavy metal removal. *Advanced Composites and Hybrid Materials*, *1*(1), 56–78. https://doi.org/10.1007/s42114-017-0004-3

Zamora-Ledezma, C., Negrete-Bolagay, D., Figueroa, F., Zamora-Ledezma, E., Ni, M., Alexis, F., & Guerrero, V. H. (2021). Heavy metal water pollution: A fresh look about hazards, novel and conventional remediation methods. *Environmental Technology and Innovation*,

22, 101504. https://doi.org/10.1016/j.eti.2021.101504

Zeng, X., Wang, Y., He, X., Liu, C., Wang, X., & Wang, X. (2021). Enhanced removal of Cr(VI) by reductive sorption with surface-modified Ti3C2Tx MXene nanocomposites. *Journal of Environmental Chemical Engineering*, *9*(5), 106203. https://doi.org/10.1016/j.jece.2021.106203

Zhang, H., Peng, L., Chen, A., Shang, C., Lei, M., He, K., Luo, S., Shao, J., & Zeng, Q. (2019). Chitosan-stabilized FeS magnetic composites for chromium removal: Characterization, performance, mechanism, and stability. *Carbohydrate Polymers*, *214*(March), 276–285. https://doi.org/10.1016/j.carbpol.2019.03.056

Zhang, L., Zeng, Y., & Cheng, Z. (2016). Removal of heavy metal ions using chitosan and modified chitosan: A review. *Journal of Molecular Liquids*, *214*, 175–191. https://doi.org/10.1016/j.molliq.2015.12.013

Zhang, S., Zhang, H., Liu, F., Yang, F., Zhou, S., Zheng, K., Chu, C., Liu, L., & Ju, M. (2019). Effective removal of Cr(vi) from aqueous solution by biochar supported manganese sulfide. *RSC Advances*, *9*(54), 31333–31342. https://doi.org/10.1039/c9ra06028f

Zhao, P., Jian, M., Zhang, Q., Xu, R., Liu, R., Zhang, X., & Liu, H. (2019). A new paradigm of ultrathin 2D nanomaterial adsorbents in aqueous media: Graphene and GO, MoS2, MXenes, and 2D MOFs. *Journal of Materials Chemistry A*, *7*(28), 16598–16621. https://doi.org/10.1039/c9ta02935d